AR-009-173

DSTO-TR-0121

DSTO

The Effects of Ferrocenic and Carborane Derivitive Burn Rate Catalysts in AP Composite Propellant Combustion: Mechanism of Ferrocene-Catalysed Combustion

T.T. Nguyen

DEPARTMENT OF DEFENCE

DEFENCE SCIENCE AND TECHNOLOGY ORGANISATION

The Effects of Ferrocenic and Carborane Derivative Burn Rate Catalysts in AP Composite Propellant Combustion: Mechanism of Ferrocene-Catalysed Combustion

T.T. Nguyen

Weapons Systems Division
Aeronautical and Maritime Research Laboratory

DSTO-TR-0121

ABSTRACT

The combustion of HTPB/AP propellants containing ferrocene-type and carborane-type burn rate catalysts was examined. The ferrocenic catalysts are good burn rate enhancers, but the carborane-type compounds showed little improvement, even at 3% catalyst concentration. An order of relative catalyst effectiveness was established for 1% catalyst concentration at 20°C. Examination reveals the enhancing effect of 1% Catocene is approximately equivalent to 0.5% Butacene. Characteristic surface features observed for the carborane-catalysed propellants contrast to those for the ferrocene-catalysed propellants. For ferrocene-catalysed combustion, the experimental evidence is in favour of a mechanism whereby the ferrocenic catalyst acts in the binder to catalyse the heterogeneous reactions between the binder and the AP at the binder/oxidiser interface. The evidence includes the following: (i) Enhanced burn rates of the Butacene propellant over the Catocene propellant, both propellants containing the same amount of iron in the ferrocenic catalysts; (ii) Fe particles dispersed in the binder of the quenched propellant surface; (iii) undercuttings along the boundaries of surface AP particles; and (iv) the convex, protruding (sometimes apparently intact) AP particle surface. There was no evidence of the catalyst promoting surface AP decomposition reactions.

DEPARTMENT OF DEFENCE

DEFENCE SCIENCE AND TECHNOLOGY ORGANISATION

Published by

DSTO Aeronautical and Maritime Research Laboratory
PO Box 4331
Melbourne Victoria 3001

Telephone: (03) 626 8111
Fax: (03) 626 8999

AR No.009-173
August 1995

APPROVED FOR PUBLIC RELEASE

DISCLAIMER NOTICE

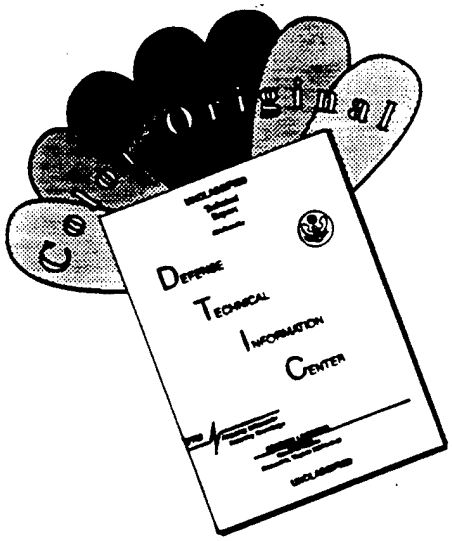

THIS DOCUMENT IS BEST QUALITY AVAILABLE. THE COPY FURNISHED TO DTIC CONTAINED A SIGNIFICANT NUMBER OF COLOR PAGES WHICH DO NOT REPRODUCE LEGIBLY ON BLACK AND WHITE MICROFICHE.

The Effects of Ferrocenic and Carborane Derivative Burn Rate Catalysts in AP Composite Propellant Combustion: Mechanism of Ferrocene-Catalysed Combustion

Executive Summary

The combustion of HTPB/AP propellants containing ferrocene-type and carborane-type burn rate catalysts was examined.

The ferrocenic derivative type catalysts included Catocene, Butacene, Hycat-6, (Ferrocenylmethyl)trimethylammonium iodide (FE-248), and 1,1'-dihydroxymethyl-ferrocene (FE-236). The carborane type catalysts included normal-hexylcarborane (NHC), and ortho-carborane. The ferrocenic catalysts are good burn rate enhancers, but the carborane-type compounds showed little improvement, even at 3% catalyst concentration. There were processing difficulties with the mixes containing the catalysts FE-248 and FE-236; they were not further examined.

An order of relative catalyst effectiveness was established for 1% catalyst concentration at 20°C.

Background ≈ o-Carborane ≈ NHC << Catocene ≈ Hycat-6 < Butacene < (Catocene + 10% PAP),

where porous AP (PAP) was included in order to determine its possible catalytic activities due to its porosity. In some instances, aluminium was also included.

For comparative assessment, the propellants containing Butacene were prepared so that they contained the same amount of iron in the ferrocenic complex as that amount of iron in the catalyst Catocene incorporated in the other respective propellants. Examination revealed that the enhancing effect of 1% Catocene was approximately equivalent to 0.5% Butacene.

There was no correlation between the burn rate enhancing effect of the additives and the sensitisation, with increasing pressure, of the AP exothermic decomposition temperature in the propellant.

Characteristic surface features observed for the carborane-catalysed propellants showed marked contrast to those for the ferrocene-catalysed propellants.

For ferrocene-catalysed combustion, the experimental evidence is in favour of a mechanism whereby the ferrocenic catalyst acts in the binder, either in enhancing the unzipping of the binder polymer, or possibly at the AP/binder interface. The evidence includes the following: (i) Enhanced burn rates of the Butacene propellant over the Catocene propellant, both propellants containing the same amount of iron in the ferrocenic catalysts; (ii) Fe particles dispersed in the binder of the quenched propellant surface; (iii) undercuttings along the boundaries of surface AP particles; and (iv) the convex, protruding (sometimes apparently intact) AP particle surface.

The arguments support the logic that the combustion is controlled by the primary diffusion flame. There was no evidence of the catalyst promoting surface AP decomposition reactions.

Fresh evidence is presented for the actual exudation of molten aluminium metal through cracks on the aluminium oxide skin formed on the burning surface of the aluminized propellants.

Author

T.T. Nguyen
Weapons Systems Division

Tam T. Nguyen holds a BSc(Hons) in Inorganic Chemistry from Sydney University, a PhD in Physical Chemistry from Newcastle University (NSW), and an MBA from Adelaide University. He transferred from CSIRO to DSTO as a Senior Research Scientist in 1986. His DSTO work includes both applied and enabling research in conventional and non-conventional composite propellant science (including ducted rocket propellants), catalysed propellant combustion, and improved performance artillery ammunition.

Contents

1. Introduction

One method of enhancing the performance of the modern missile system is to increase the burn rate of the rocket motor. This is particularly important for composite propellant motors, i.e. those based on ammonium perchlorate (AP) with an inert polymeric binder, where metal containing catalysts are commonly used as burn rate enhancers.

Numerous mechanistic studies have shed some light, *albeit* not totally satisfactory, as to how these catalysts function. A great deal of effort has been focussed on the relative importance of the role played by the AP oxidiser and the binder. One school of thought advocates that burn rates of composite propellants are determined by the burn rates of the oxidiser AP and its catalyzed decomposition reactions [1-4]. Another puts more emphasis on the binder and its catalyzed heterogeneous reactions with the oxidiser [4,5]. A long standing controversy has been the question as to whether the catalyst promotes gas-phase reactions or condensed phase (i.e. surface and sub-surface) reactions in burn rate enhancement [3,4,6].

In favour of gas-phase reactions, Pittman [7] suggested that iron-containing catalysts such as ferrocenes probably act in the gas phase to increase the rate of decomposition of perchloric acid or the rates of reactions of its initial decomposition products. Burnside [8], Pearson [9], and Bakhman et al. [10] believed that iron oxide catalyzes gas-phase reactions of AP decomposition products, and the burn rate enhancement was correlated to the specific surface area of the solid catalyst, chamber pressure, and the particle size of the AP. Rastogi et al. [11] suggested that the actual species catalyzing the burn rates was the oxide derived from the original metal salt additive which functions by promoting the gas-phase reactions on the surface but not the exothermic reactions in the condensed phase.

The notion that catalysed condensed phase reactions are important can be related to the importance of the heterogeneous reactions between the binder and AP, or to the binder decomposition itself. Evidence for condensed phase reactions between AP and the binder was shown by the existence of a phase transition zone of AP in the sub-surface region of the burning propellant [12-14]. The transition zone occurs within 1 mm of the surface, and the orthorhombic and cubic phases of AP coexist over a time-dependent 50-μm zone which subsequently become the advancing combusting surface. Thus conditions exist in the condensed phase for the decomposition of AP and binder and the heterogeneous reactions between their products [4].

Because the time scale for condensed phase reactions is in the order of 10^{-3} s, which is longer than the characteristic transport/mixing time (10^{-4} s) in the burning of composite propellants, condensed-phased reactions were argued to be the major rate-controlling mechanism [15].

By examining the scanning electron microscopy (SEM) of quenched propellant surfaces, Krishnan et al. [16-18] concluded that iron oxide and copper chromite catalysts enhance the propellant burn rates by promoting heterogeneous surface and

sub-surface reactions between the binder and oxidiser. Such a conclusion was in agreement with earlier observations using sandwich propellants by Price et al. [19,20]. Kishore et al. [3,21,22] confirmed that definite evidence for condensed-phase reactions was the identification of peroxide intermediates by chemical analyses and infrared spectroscopy of quenched propellants.

A model was put forward [23] to incorporate condensed phase reactions where both AP and the binder decompose in the solid phase, and the products mix and interact in the interstices between the AP particles and the binder.

While the evidence is strong for condensed phase reactions between the binder and oxidiser, evidence was not convincing for binder degradation enhanced by the presence of catalyst. On the one hand, binder thermal degradation has been claimed [24] to be the rate-limiting step in HTPB/AP combustion catalyzed by copper containing additives. Copper chromite was found to increase the burn rate when it was premixed into the binder [4,25], but not when it was premixed into the AP. On the other hand, no augmented binder pyrolysis was observed when catalysts known to enhance propellant burn rates were used [1,5]. Cohen, Fleming and Derr [5], and Jones and Strahle [26] showed that changes in the kinetics or heats of degradation of the polymeric binders do not have a significant effect on propellant burn rates. Such negative results were interpreted as inferring the catalyst affects gas-phase AP decomposition reactions [5]. It is important to note that some of these studies employed thermal analysis techniques under conditions far removed from actual conditions prevailing in propellant combustion. Caution has been raised over the application of decomposition data to deflagration situations because of the widely differing conditions between the decomposition regime and the deflagration regime [27].

The question of a dual role has also been mentioned. One study [28] suggested copper chromite catalyst accelerates the decomposition of the oxidiser AP as well as promotes the oxidation of the fuel through heterogeneous reactions. Yet another study [26] showed that copper chromite does not promote heterogeneous reactions with solid fuel binder, nor modify binder pyrolysis, but it possibly enhances gas-phase reactions by its presence in the interface between the AP and binder.

Because of the complex and confusing literature mentioned above, the present study examined the catalyzed combustion of HTPB/AP propellants with a view to obtaining a better understanding of the propellant burning surfaces, their combustion behaviour and the prevailing mechanism of burn rate catalysis. The HTPB/AP propellants studied contained two types of catalysts: ferrocene derivatives and carborane derivatives. In some instances, aluminium was also incorporated. An order of relative catalyst effectiveness is established. More importantly, evidence is presented from burn rate measurements and burning surface characteristics that the ferrocenic catalysts act in the binder to promote the heterogeneous reactions between the binder and the AP. Condensed-phase reactions at the binder/AP interface are found to be important for catalyzing the primary diffusion flame, while no evidence was found for catalyzed decomposition reactions of AP on the burning surface.

The combustion behaviour of iron and aluminium particles was also examined. Inferrence on aluminium combustion was made in the literature, but mostly indirectly based on laboratory tests under simulated conditions. In the present study, the actual exudation of molten aluminium metal was observed through cracks on the aluminium oxide skins. For the ferrocene containing propellants, the surface species were identified to be iron oxides undergoing vigorous decomposition reactions on the burning surface.

2. Experimental

(1) Materials:

Bimodal blends of AP were used, consisting of a medium-sized (200 μm) fraction and a small-sized (20 μm) fraction. This combination was recommended as offering an optimum AP particle size width distribution [29] to enable the best possible reduction of propellant burn rate temperature sensitivity [30]. The propellant formulations studied were of the conventional type in terms of binder and oxidiser weight fractions and had typical temperature sensitivity and pressure exponent values for HTPB/AP systems.

The materials used as propellant ingredients are described in Table 1.

Table 1: Propellant Ingredients

Materials	**Sources**
HTPB R45M	Elf-Atochem
Ammonium Perchlorate	Kerr-McGee Chemical Corp.
Porous Ammonium Perchlorate	DSTO from Kerr-McGee
DDI 1410	General Mills
Catocene	Thiokol
Butacene® 800	SNPE
Hycat 6	Arapahoe
n-Hexyl Carborane	Gallery Chemical
FE-236	ROC/RIC
FE-248	ROC/RIC
Tetraethylsilane	Aldrich Chemical Co.
Aluminium VM H60	Valley Metallurgical
Boron	BDH
o-Carborane	Aldrich
Antioxidant AO2246	Nonox

The ferrocenic derivative type catalysts included Catocene, Butacene, Hycat-6, (Ferrocenylmethyl)trimethylammonium iodide (FE-248), and 1,1'-dihydroxymethyl-ferrocene (FE-236). Catocene is a dark orange viscous liquid, and contains two

ferrocenic moieties in its molecule. Butacene is a HTPB pre-polymer with a single ferrocenic unit grafted on to the polymer backbone. Hycat-6 is structurally analogous to Catocene with the two methyl groups in the latter replaced by hydrogens. The FE-248 and FE-236 are powders, each containing a ferrocenic unit.

The carborane type catalysts included normal-hexylcarborane (NHC), and ortho-carborane. NHC is a colourless liquid, and o-carborane is a white crystalline solid. Porous AP (PAP) was prepared in-house (see below) from commercial batches of AP, in order to determine its possible catalytic activities due to its porosity.

(2) Preparation of PAP

PAP was prepared by the oven baking method as described by Klager et al [31]. A layer of about 0.5 cm thick of particulate (200 μm) AP was spread evenly on a tray and baked in a vented oven at 245°C. The AP was partially decomposed at this temperature, leaving a residue of about 70% by weight which was still pure AP but possessing a high degree of porosity.

Characteristic thermal decomposition and evidence of porosity of the PAP was confirmed by DSC, TGA, and SEM. The PAP was coated with a solution of an adduct of divinylbenzene in hexane [31]. The coating seals the outer pores and prevents filing the tunnels within the PAP with propellant binder during manufacture of the propellant. It also prevents re-conversion of PAP to AP upon exposure to water vapour.

(3) Propellant Processing and Manufacture

The propellants were manufactured in 500 g batches using an anchor blade mixer equipped with vertical breaker bars. All mixes were performed under reduced pressure at 60°C. After mixing, the propellant was top cast under reduced pressure into a rectangular mould and subsequently cured for one week at 60°C. The castability of the propellant and the rate of the early stage of the cure reaction was determined by measuring the viscosity of the propellant as a function of time. A Haake RV3 viscometer with a cup and rotor sensor was used for these measurements. Particle size distributions were measured on a Malvern Mastersizer/E.

Formulations of the propellants containing different types of catalysts at various concentration levels are summarised in Table 2.

(4) Strand Burn Rate Measurements

The cured propellant slabs were machined into strands of dimensions 175 x 5 x 5 mm. The strands were inhibited with coatings of phenolic epoxy resin, or polyvinyl acetate paint. For the propellants which proved difficult to burn, the strands were dipped in epophene and wrapped in glass tape.

Table 2: Propellant formulations (weight %) containing various catalysts at different concentrations

Baseline propellant	Catocene concetration					
	No catalyst	(0.2%)	(0.5%)	(1%)	(3%)	(3% with 5% Al)
HTPB	13.79	13.79	13.79	13.73	13.79	13.79
AP (200 μm)	53.95	53.82	53.63	53.30	52.00	48.75
AP (20 μm)	29.05	28.98	28.87	28.70	28.00	26.25
Catocene	-	0.20	0.50	1.00	3.00	3.00
DDI	3.21	3.21	3.21	3.27	3.21	3.21
Aluminium	-	-	-	-	-	5.00
	Hycat 6 concentration					
	(0.2%)		(1.0%)		(3%)	(3% with 5%Al)
HTPB	13.79		13.79		13.79	13.79
AP (200 μm)	53.82		53.30		52.00	48.75
AP (20 μm)	28.98		28.70		28.00	26.25
Hycat 6	0.20		1.00		3.00	3.00
DDI	3.21		3.21		3.21	3.21
Aluminium	-		-		-	5.00
	Butacene concentration					
		(0.5%)		(1%)		(3%)
HTPB		12.42		11.18		5.91
Butacene		1.47		2.95		8.83
AP (200 μm)		53.95		53.95		53.95
AP (20 μm)		29.05		29.05		29.05
DDI		3.11		2.87		2.26
	PAP concentration					
	(5%)		(10%)		(15%)	(20%)
HTPB	13.79		13.79		13.79	13.79
PAP	5.00		10.00		15.00	20.00
AP (200 μm)	48.95		43.95		38.95	33.95
AP (20 μm)	29.05		29.05		29.05	29.05
DDI	3.21		3.21		3.21	3.21
	NHC concentration					
	(0.2%)	(0.5%)		(1%)	(3%)	(3% with 5%Al)
HTPB	13.79	13.79		13.79	13.79	13.79
AP (200 μm)	53.82	53.63		53.30	52.00	48.75
AP (20 μm)	28.98	28.87		28.70	28.00	26.25
NHC	0.20	0.50		1.00	3.00	3.00
DDI	3.21	3.21		3.21	3.21	3.21
Aluminium	-	-		-	-	5.00

The strands were burned in a Nitrogen pressurised bomb over a range of pressure from 2 to 18 MPa. Two fusion wires embedded in the propellant strand and connected to a timing circuit enabled the burn rate to be determined.

All burn rate measurements were at 20°C. Reproducibility of burn rate results was ensured by duplicate (or triplicate) measurements of burn rate at the same pressure. Burn rates as a function of pressures were plotted and the curves of best fit through the data points were obtained by least square regression and described by polynomial expressions.

(5) Interrupted Bomb

An interrupt bomb, constructed in the Division [32a] from a design by the Naval Weapons Center [32b], was employed in the experiments involving quenching of burning propellants. The quenched propellant was examined by scanning electron microscopy.

A propellant strand (length 40 mm, cross section 5 x 5 mm) was burned in the bomb at a set pressure in the range 2 to 10 MPa, and quenched by rapid depressurisation of the nitrogen. A stack of Mylar disks (disk thickness 0.13 mm) was used as diaphragm in the combustion chamber. The propellant strand, mounted at the opposite end of the bomb, could be ignited by an igniter wire inserted through it. A nichrome wire, sandwiched between the mylar disks, was heated by a triggered capacitor discharge. The hot wire caused immediate rupture of the Mylar disks, leading to a rapid drop in the chamber pressure which extinguished the propellant combustion. The number of mylar disks to be used was dependent on the bomb pressure under which the propellant burned [32]. The rate of depressurisation was estimated to be 140, 210, 500, and 700 MPa/s at the bomb pressures of 2, 3, 7 and 10 MPa to ensure that propellant burning was completely and permanently extinguished. Some alteration of the surface structure may have resulted from the quenching process. However, for other similar experimental systems it has been re-affirmed by Boggs, Derr and Beckstead [33] that the marked correlation between the structures of the burning samples observed in high speed, high magnification cinephotomicrography and the structure of the samples quenched by rapid depressurisation and examined by SEM indicated that any artifacts due to the quenching would be of minor importance.

(6) DSC Measurements

DSC measurements were performed on a Du Pont Instrument 910 Differential Scanning Calorimeter. Calibration was checked using indene as standard. A Du Pont high pressure cell was used for DSC measurements up to 6.9 MPa. Sample size was approximately 2 mg, and scan rate was 10°C per minute.

(7) Scanning Electron Microscopy

Scanning electron microscopy (SEM) was carried out using a Jeol JSM 35 scanning electron microscope which had a Tracor Northern microprobe attachment for qualitative element identification by Energy Dispersive Analysis. X-ray digital images of elements were constructed by a Tracor Northern X-Ray Analyser coupled to the Jeol

JSM 35. The X-Ray Analyser used a Flexitran program called the Image Processing Program (IPP) to construct digital elemental X-ray maps according to the intensities of X-rays produced by the electron microscope. Associated Tracor Northern software was used for the microscan calibration program and for the microscan digital beam controller.

A portion of the burned propellant strand, obtained by quenching in the interrupt bomb, was cut and mounted on a sample holder for SEM examination. In order to prevent surface charging, i.e. build-up of electrostatic potential on the non-conducting propellant surface, the surface was coated with a thin layer of gold (a few hundred Angstrom thick) by vacuum deposition. Re-coating was found to be necessary when some samples, after being exposed in the intense electron beam for a sufficiently long time, started to produce a display which showed interfering wide horizontal streaks. The sample penetration depth of SEM depends on the energy of the primary electron beam, and for non-conducting propellants is expected to be below 0.5 μm.

(8) X-Ray Photoelectron Spectroscopy

Preliminary X-ray Photoelectron Spectroscopy (XPS) of quenched propellant strands was examined. The ESCA system used was a Perkin-Elmer (Physical Electronics Division) Model 5100 ESCA/SIMS. It incorporated a hemispherical analyser which had an energy range 0 to 4800 eV and a practical resolution of 0.5 eV. The photoelectrons analysed by the detector in XPS originate from a sample cross sectional area of approximately 4 x 8 mm.

The system was run by a Perkin-Elmer 7000 series computer using the ESCA software package. The analyser was calibrated using the Ag 3d peak for the electron multiplier voltage. The pass energy of the analyser was calibrated using the Au 4f and Cu $2p_{3/2}$ peaks. XPS is a technique providing information about elemental and chemical state (e.g. valency, oxidation) of the first 30-Angstrom depth of a solid surface. The applicability of XPS to propellant combustion studies has been recently reviewed [33].

3. Results

3.1 Burn Rates

(a) Catocene Propellants

Burn rate results at 20°C for propellants containing 0.2, 0.5, 1 and 3% Catocene catalyst are detailed in Table 3. Polynomial expressions were obtained to describe the best fit curves for burn rates as a function of pressures in the range 2 to 18 MPa. The burn rate curves are shown in Figure 1. The propellant containing 0.2% Catocene shows burn rate enhancements up to approximately 30% with respect to the non-catalyzed reference propellant. At 1% Catocene concentration, a burn rate increase of almost 80%

was observed. The enhancements however are not proportional to the catalyst concentrations. Some apparent plateau burn rate regions were observed for the 0.2, 0.5 and 3% Catocene propellants.

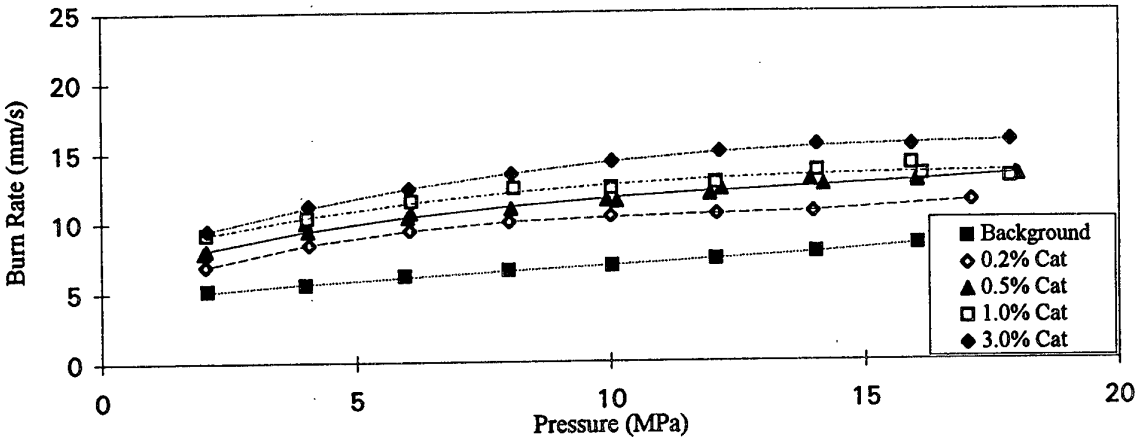

Figure 1: Burn rates of propellants containing 0.2, 0.5, 1 and 3% Catocene.

Burn rate results for propellants incorporating Catocene (0.5 and 1%) and with 10% of the 200 μm AP replaced by PAP are shown in Figure 2. The addition of PAP significantly enhanced the burn rates of the Catocene propellants; increases of up to 50% were observed in the 8-10 MPa region.

Table 3: Burn Rates (mm/s) as a Function of Pressure of Propellants Containing Various Catalysts at Specified Concentration (weight %)

Pressure (MPa)	No Catalyst	Catocene					Butacene			NHC	
		0.2%	0.5%	1%	3%	3%+5% Al	0.5%	1%	3%	3%	3%+5% Al
2	5.08	6.92	7.95	8.45	9.38	8.79	7.77	8.97	13.60	5.64	5.40
4	5.62	8.52	9.39	9.84	11.04	10.44	9.54	10.80	14.75	6.43	5.58
6	6.08	9.61	10.41	10.86	12.39	11.72	10.79	12.35	16.29	6.86	5.86
8	6.48	10.32	11.10	11.61	13.47	12.68	11.62	13.66	18.13	7.10	6.23
10	6.87	10.78	11.58	12.18	14.29	13.37	12.17	14.77	20.15	7.31	6.67
12	7.27	11.10	11.97	12.65	14.89	13.84	12.55	15.75	22.25	7.66	7.17
14	7.74	11.42	12.39	13.11	15.30	14.16	12.89	16.63	24.32	8.31	7.69
16	8.29	11.84	12.95	13.66	15.55	14.36	13.30	17.47	26.26	9.43	8.24
18	8.97	12.50	13.77	14.39	15.66	14.52	13.91	18.32	27.97	11.18	9.79
20	9.80	13.51	14.96	15.39	15.67	14.67	14.84	19.23	29.34	13.73	9.23

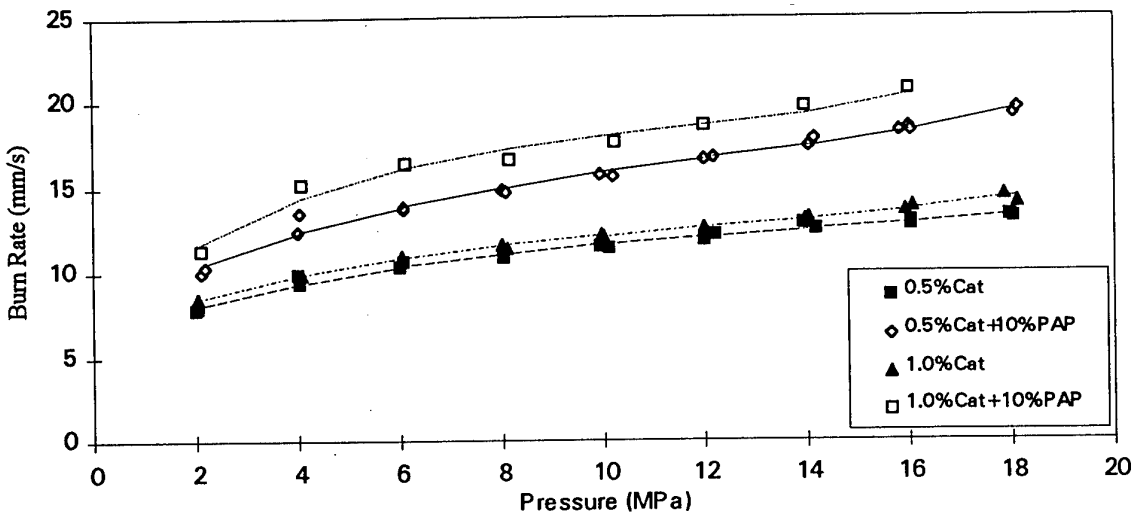

Figure 2: Burn rates of propellants containing Catocene and PAP (PAP replacing 10% of the 200 μm AP).

(b) Hycat-6 Propellants

Burn rates for the propellant containing 1% Hycat-6 are compared with the propellant containing 1% Catocene in Figure 3; they are very similar. Measurements with propellants containing Hycat-6 at several other concentrations confirmed that Hycat-6 and Catocene have nearly identical burn rate enhancing effectiveness. As mentioned earlier, the Hycat-6 molecule is chemically very similar to the Catocene molecule. The present findings are in agreement with previous results [24] showing propellant burn rates are insensitive to alkyl substitution in metal chelate catalysts.

(c) Butacene Propellants

The propellants containing 0.5, 1 and 3% Butacene were manufactured so that they contained the same amount of iron as that in the propellants containing 0.5, 1 and 3% Catocene. The Butacene propellant burn rates are summarised in Table 3, and compared with the Catocene propellant burn rates in Figure 4. It is significant that the Butacene propellant burn rates are always higher than the corresponding Catocene propellant burn rates. These results are important in the following discussion on the location of the catalytic active sites and the mechanism of ferrocene-catalyzed combustion.

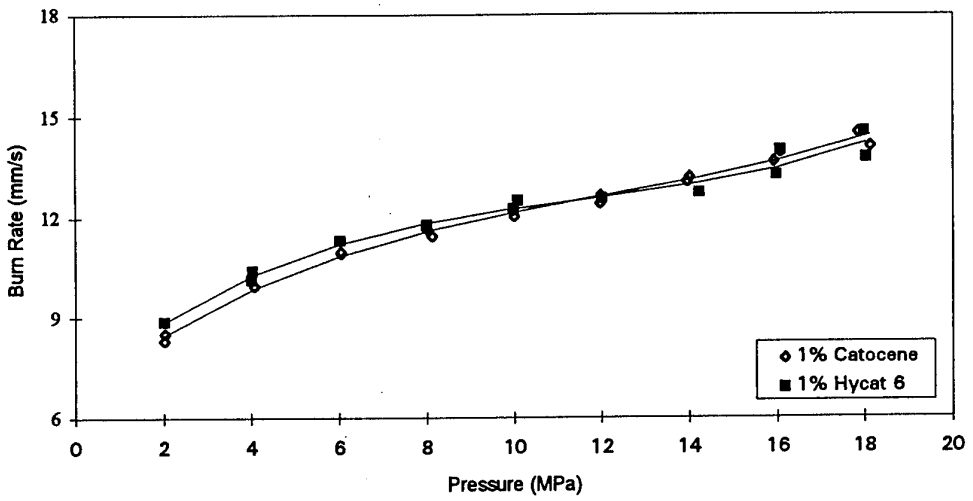

Figure 3: Comparison of burn rates of propellants containing 1% Hycat-6 and 1% Catocene.

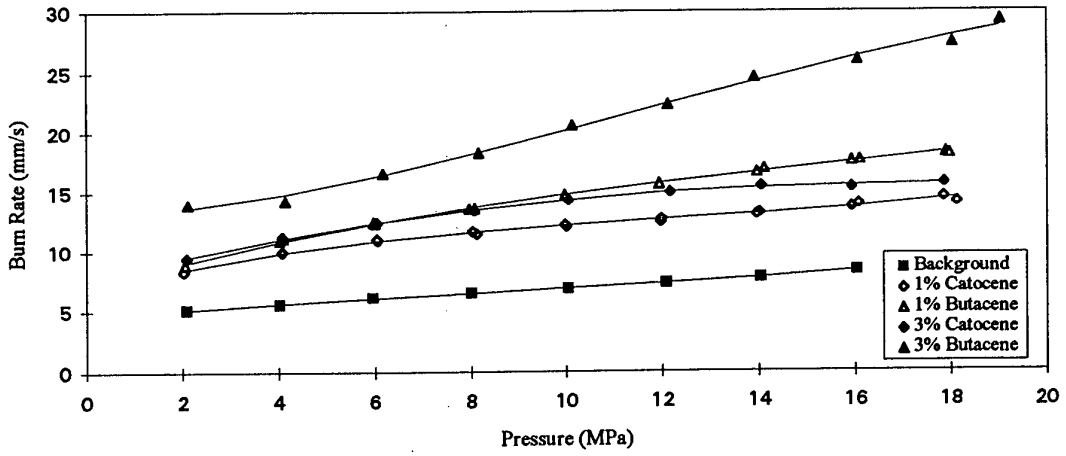

Figure 4: Comparison of burn rates of propellants containing Catocene and Butacene.

The molecular structure of Catocene and Butacene are shown in Figure 5. Since Butacene consists of a single ferrocenic moiety and a pre-polymer HTPB joined together through a silane-type linkage, the possible enhancing effect of the silane-type linkage was examined. Tetraethylsilane (TES) was used, and the burn rates of the propellant containing 1% of this compound was compared with those of the background uncatalysed propellant; see Fig 6. The two burn rate curves are almost identical, indicating that there is no enhancing effect from the silane linkage. Thus it can be comconluded that the observed enhanced burn rates of the Butacene containing propellants originate from the catalytic effect of the ferrocenic moiety alone.

(a) Catocene
(2,2-bis[ethylferrocenyl]propane)

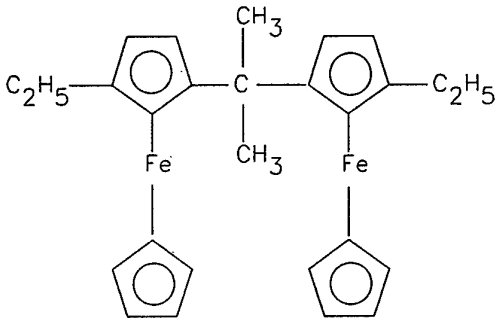

(b) BUTACENE®

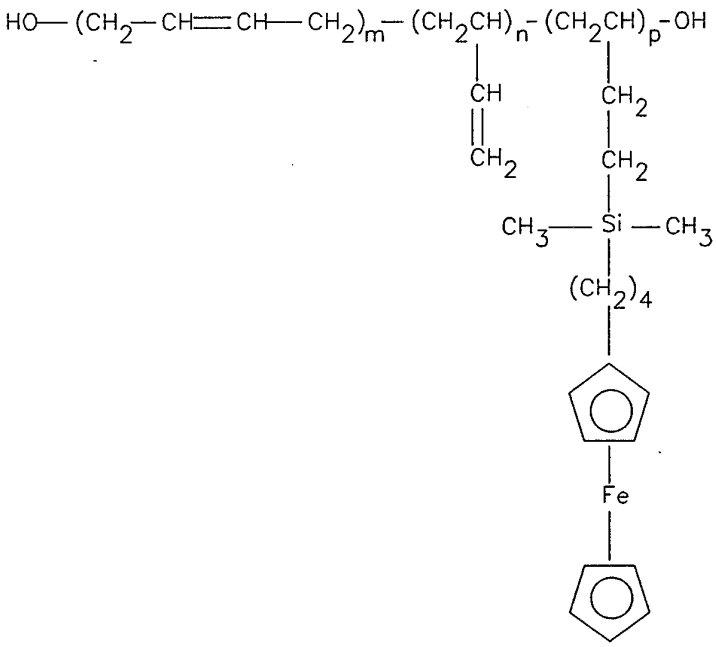

Figure 5: Chemical structure of Catocene and Butacene.

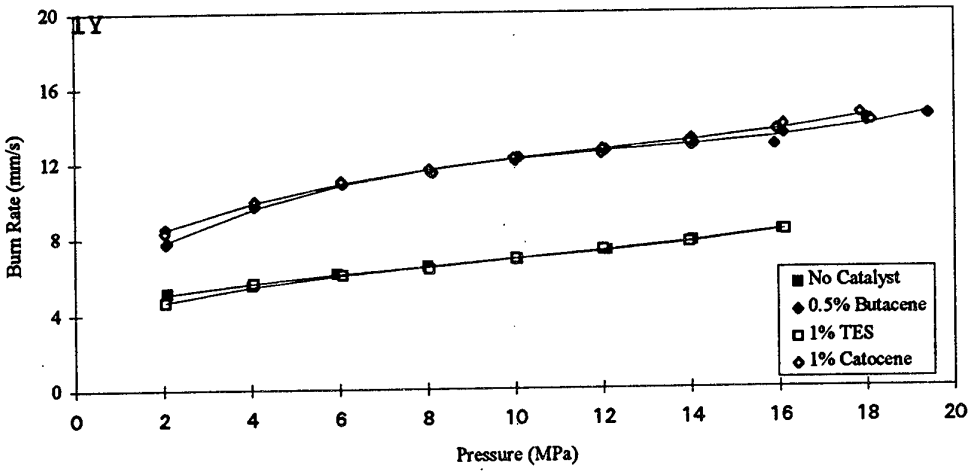

Figure 6: Comparison of burn rates of the 1% Tetraethylsilane propellant with the baseline propellant, and of the 1% Catocene propellant with the 0.5% Butacene propellant.

(d) FE-236 and FE-248 Propellants

At 1% concentration, FE-236 appears to be a marginally poorer catalyst than Catocene at pressures less than 10 MPa, but its effectiveness decreased substantially at pressures higher than 10 MPa. There appeared to be no significant differences between burn rates of the 0.5 and 1% FE-236 propellants.

Burn rates of the propellants containing 0.5 and 1% FE-248 show poor reproducibility, and no discernible patterns could be established. Strong scatter of the data points (Figure 7) probably resulted from processing difficulties encountered with the propellant mixes. Degassing occurred during casting, and particle sedimentation caused the propellant slab to have a non-uniformly coloured appearance. While FE-236 is a covalent compound, FE-248 is an ammonium iodide salt, and ionic interaction with the AP could probably have caused separation of the mix into two distinct phases. Propellants containing these catalysts were not examined further.

(e) Boron-Containing Propellants

Burn rate results at 20°C for propellants containing NHC, o-Carborane and boron are shown in Figure 8. Compared to the reference propellant, there were only marginal enhancements for the propellants containing 1% and 3% NHC. The propellant incorporating 1% o-Carborane also shows very similar results to that containing 1% NHC. Thus o-Carborane and NHC are not effective catalysts for these propellant formulations. Boron as 2% metal additive appeared to be a better catalyst, showing burn rate enhancements over those of the propellant containing 3% NHC.

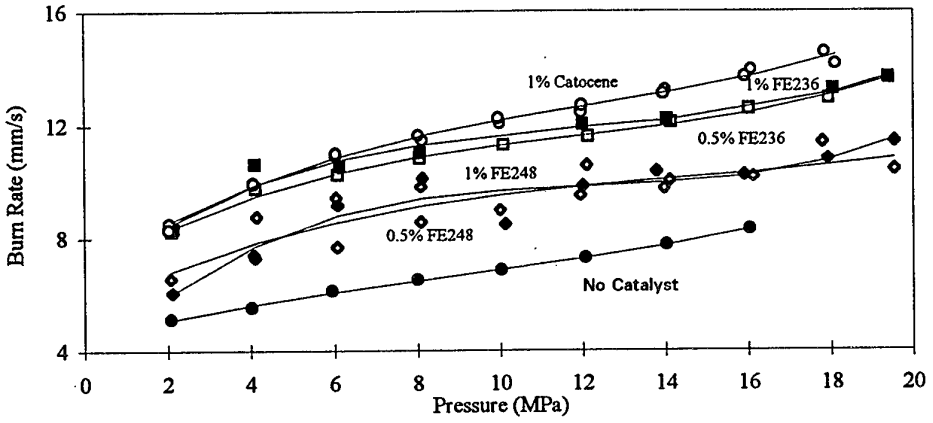

Figure 7: Burn rates of the propellants containing the ferrocenic catalysts Catocene, FE236 and FE248.

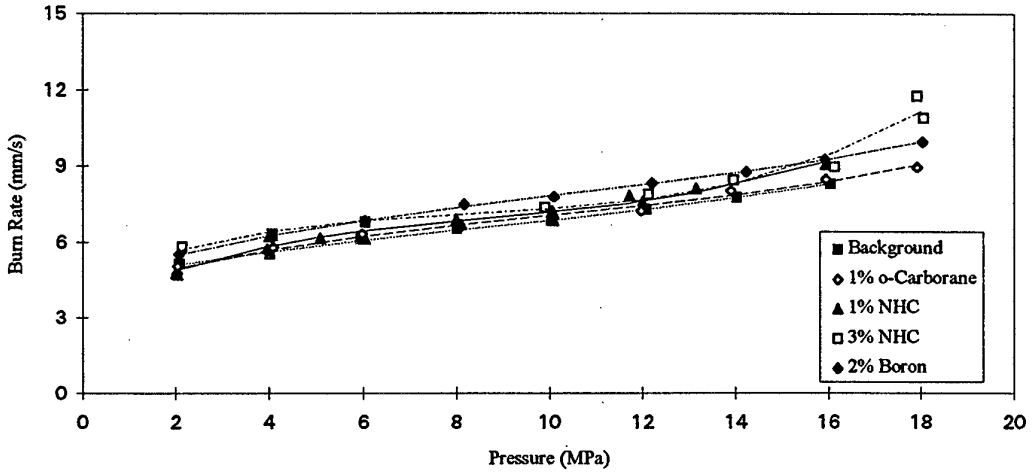

Figure 8: Burn rates of propellants containing NHC, ortho-Carborane and boron.

(f) Aluminized Propellants

Figure 9 shows the burn rates of aluminized propellants containing Catocene and NHC compared to the non-aluminized, catalyzed propellants. A consistent trend is clear. The effect of added aluminium was to lower the burn rates from those of the respective non-aluminized propellant.

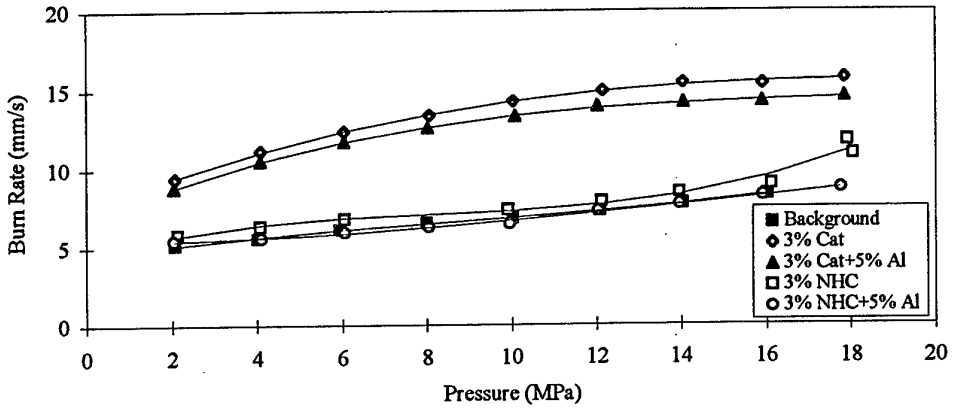

Figure 9: Burn rates of aluminized propellants containing Catocene and NHC compared to corresponding non-aluminized propellants.

3.2 Thermal Decomposition

The DSC plots for PAP at pressures from ambient to 6.9 MPa all contain a sharp endotherm near 245°C, and two pressure-dependent exotherms. The endotherm near 245°C corresponds to the well-characterized phase transition of AP from orthorhombic to cubic structure, and the pressure-dependent overlapping exotherms with peaks in the range 280-440°C correspond to the two-stage thermal decomposition of AP. The exotherms appeared near 373°C at ambient pressure, increased to 425°C at 2 MPa, but declined to 381°C at 4 MPa and further to 375°C and 367°C at 5.6 and 6.9 MPa, respectively. Thus pressures higher than 2 MPa appeared to sensitize the thermal decomposition of PAP.

High pressure DSC results were also obtained for the 200 μm AP. The exothermic decomposition temperature of AP is pressure-dependent, but there was no apparent trend of sensitization at high pressures. The exothermic decomposition temperatures of AP in AP-based propellants containing various catalysts are summarized in Table 4.

As summarised in Figure 10, at pressures higher than 4 MPa, the propellant containing 10% PAP (which partially replaced the 200 μm AP) shows exothermic decomposition temperatures in DSC plots more similar to those of oxidiser AP than of PAP. The propellant containing 1% Catocene (without PAP) shows AP exothermic temperatures more sensitised at high pressures, appearing to follow the same trend as that of the Butacene propellant, NHC propellant, and o-Carborane propellant. However, the behaviour of the propellant containing 1% Catocene (with 10% PAP replacing AP) seems to follow the same pattern as that of the propellant containing 10% PAP. Thus the effect of the oxidiser PAP and AP seemed to be dominating over that of Catocene in the (1% Catocene + 10% PAP) propellant.

Table 4: Exothermic Decomposition Peak Temperature (°C) of AP as a Function of Pressure in Various Propellants

Pressure (MPa)	Oxidiser		AP/HTPB Propellant					
	AP	PAP	10% PAP	1% Catocene + 10% PAP	1% Catocene	1% Butacene	1% NHC	1% o-Carborane
ambient	437	373	361	342	344	348	386	395
2	439	425	407	391	360	345	345	453
4	401	381	418	408	380	357	363	375
5.6	408	375	-	-	-	-	368	367
6	-	-	420	422	377	362	-	
6.9	411	367	-	-	-	-	371	365

As shown in Figure 10, o-Carborane, NHC, Catocene and Butacene all seemed to have a sensitizing effect on the exothermic decomposition temperature of AP in the respective propellants at high pressures.

3.3 Scanning Electron Microscopy (SEM)

(a) Non-Aluminized Propellants

SEM micrographs of the quenched burning surfaces of the propellants containing the ferrocenic catalysts all show undercuttings, to varying degrees, along the boundaries of AP surface particles where the oxidiser is in contact with the binder. This observation suggests that heterogeneous reactions are occurring at the interfacial region on the burning surface [16-18,34]. For the propellant containing 0.5% Catocene catalyst, or 0.5% Butacene catalyst, the undercuttings were quite pronounced at both low (2 MPa) and high (10 MPa) pressures; see Figure 11a and b.

A characteristic feature of the ferrocenic catalysed propellants is the convex shape of the AP particle surface on the burning propellant. The protruding AP surface suggests that the regression rate of the propellant as a whole is faster than that of the oxidiser particles. The burning surface of the larger oxidiser particles were lagging behind the flame front of the regressing surface. Careful examination revealed the surface of the smaller, 20 μm AP particles, was mostly convex, though not to the same extent as for the larger 200 μm AP. For the Catocene and Butacene containing propellants this characteristic was observed throughout the pressure range 2 to 10 MPa.

Another characteristic was the white frothy areas observed near the middle of the AP particle surfaces, indicating the presence of gaseous decomposition products from intense surface/sub-surface reactions. In particular, on the Butacene containing propellant more white frothy areas were noticed at lower pressures than at high pressures, and they tended to spread widely over the binder surface.

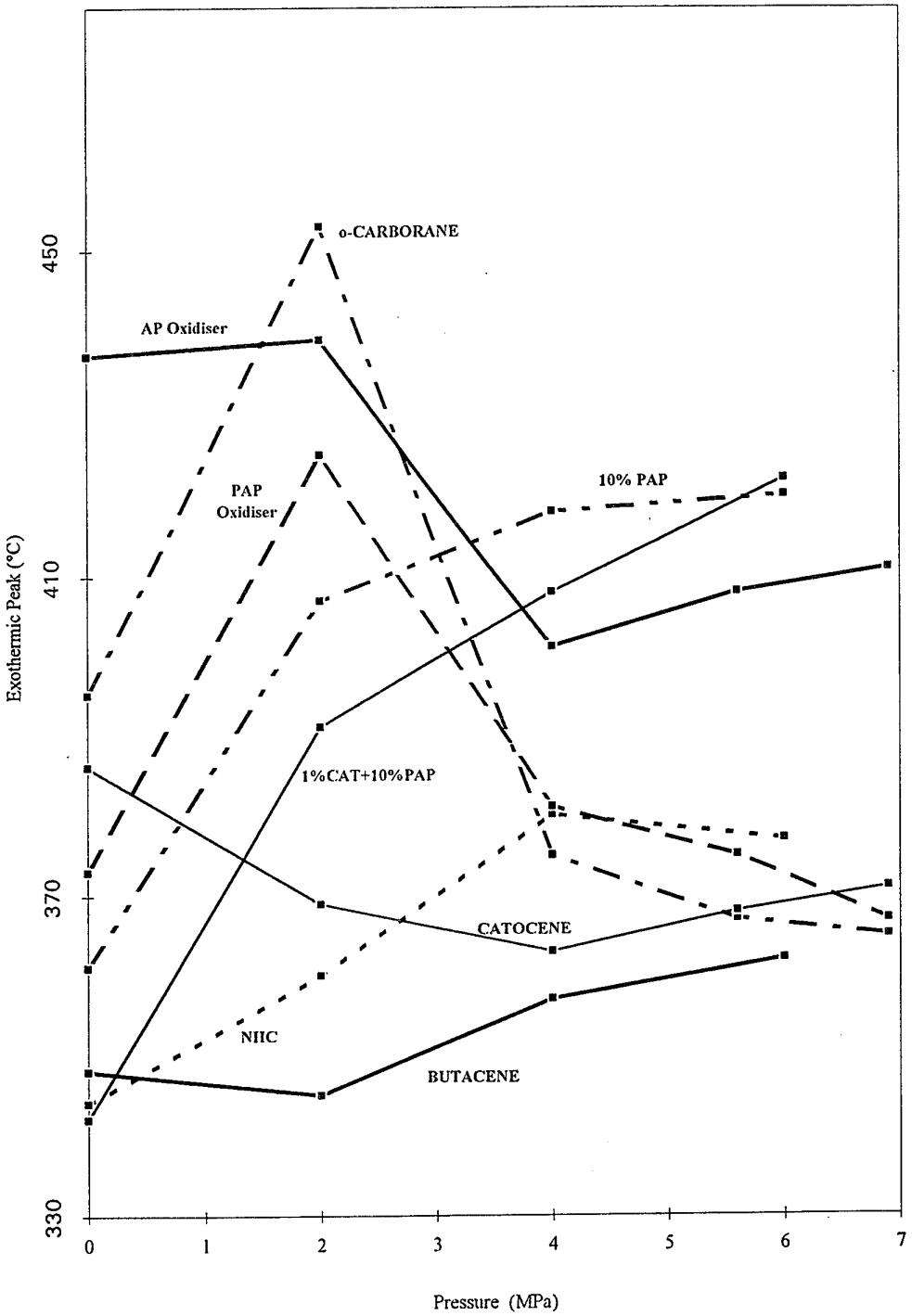

Figure 10: Exothermic decomposition temperatures of AP in propellants containing various catalysts as a function of pressure.

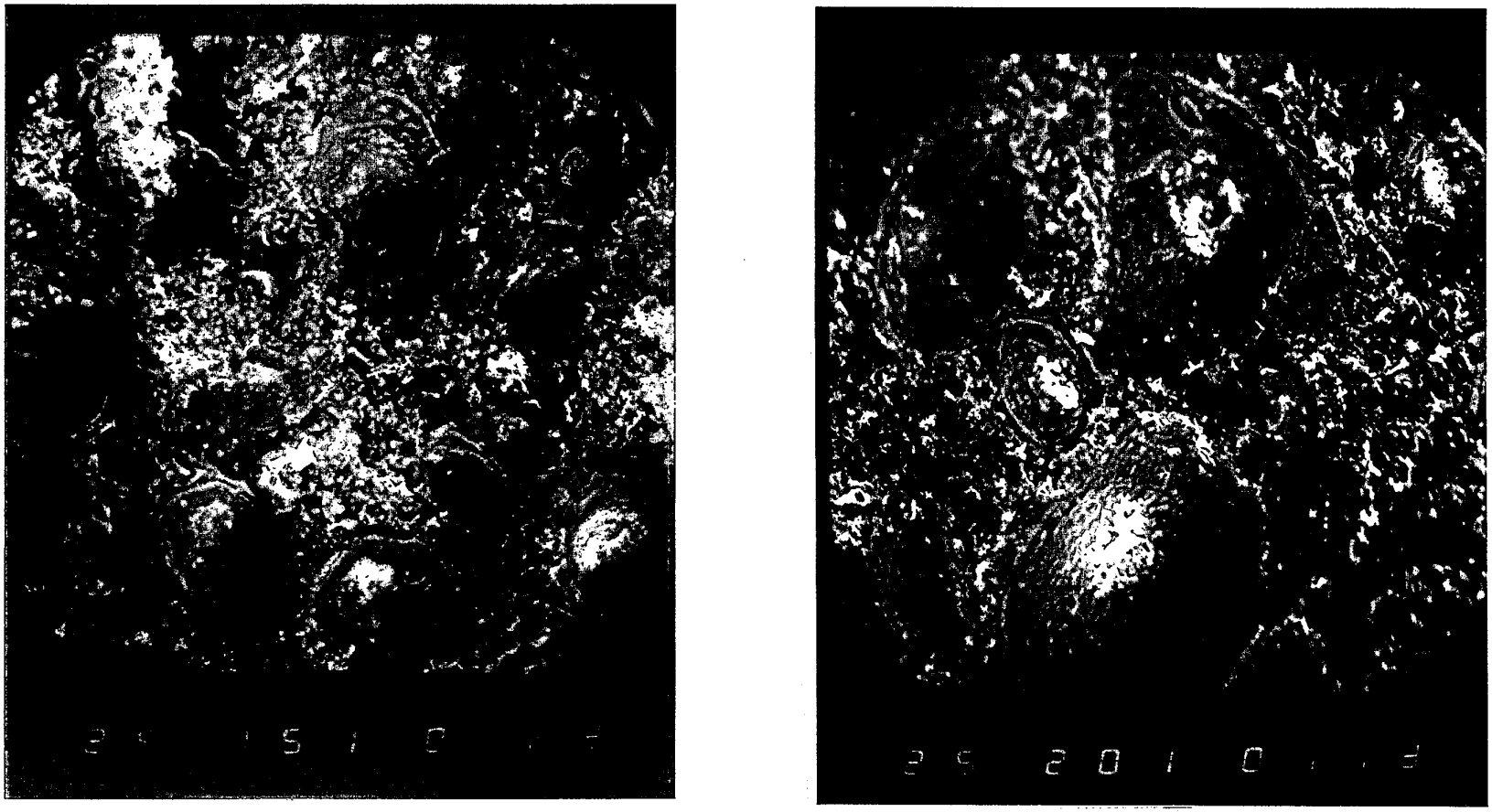

Figure 11: SEM photographs of a burning AP/HTPB propellant surface containing Butacene catalyst (0.5% concentration) at (a) 2 MPa, and (b) at 10 MPa, showing protruding surfaces of AP particles, white frothy areas at the middle of AP particle, and undercuttings along the AP particle boundaries.

Figure 12: SEM photograph of an AP/HTPB propellant containing a carborane catalyst and aluminium burning at 3 MPa.

In sharp contrast, the surfaces of the larger AP particles in the carborane containing propellants were concave at both low and high pressures; see Figure 12. This observation suggests that the binder was burning at a slower rate than the oxidiser and is consistent with the much slower regression rates observed for the NHC and o-Carborane containing propellants. Further, the burning surface of carborane containing propellants were distinctly different from that of the ferrocene-catalysed propellants; it had a "rocky" and "pebbled" appearance, and was covered by a layer of viscous binder melt. There was little evidence of those white, intensely frothy areas as observed on the ferrocenic propellants. The existence of a binder melt on the propellant surface has been noted in previous work [17,34,35]. Such a melt layer, spreading widely on the

carborane catalysed propellant surface, would inhibit and/or extinguish surface-initiated reactions and therefore suppress burn rates.

Under high magnification, the SEM micrographs (Figure 13) of the ferrocenic catalysed propellants show aggregations of vigorously reacting iron compounds displaying intensely frothy, white, blooming areas. A careful search revealed no evidence of well-defined particle shape as that observed for aluminium in the aluminized propellants (see below). XPS of the quenched propellants showed the Fe 2p spectra occurring at a binding energy of 712 eV, attributable to iron oxides in the form of Fe_2O_3 and/or Fe_3O_4.

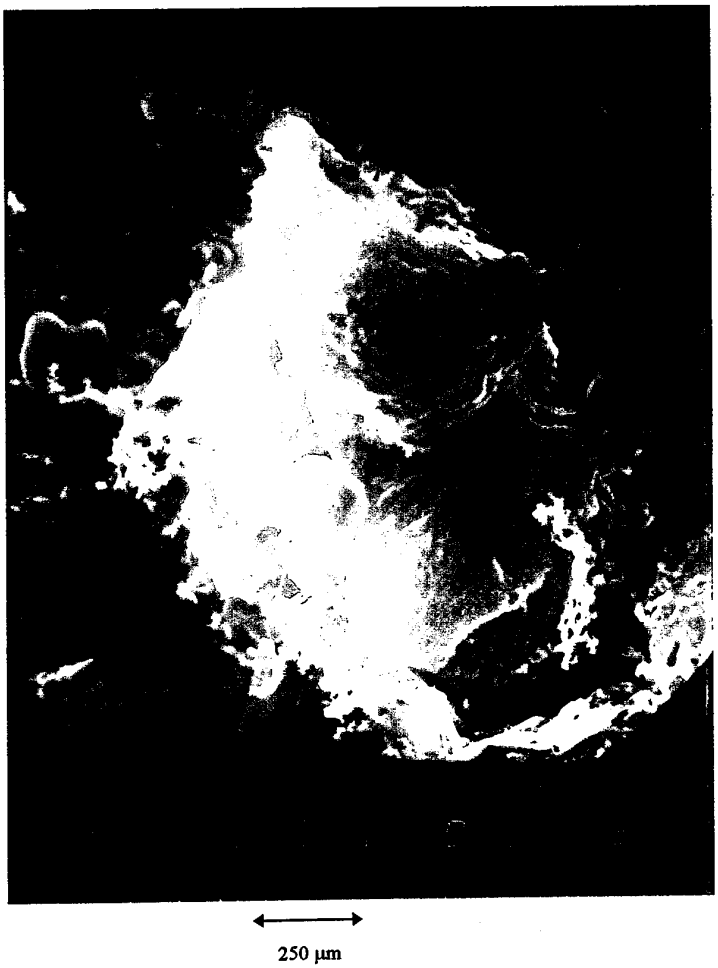

Figure 13: SEM photograph showing vigorous decomposition reactions of a ferrocenic catalyst in an AP/HTPB propellant burning at 3 MPa.

(b) Aluminized Propellants:

The present work presents some new, direct information about the combustion behaviour of aluminium in AP-based composite propellants. The SEM photographs showed the extinguished aluminized propellant surface contained egg-shaped aluminium agglomerates which resulted from the coalescence of aggregates of slow burning aluminium particles after emerging from the burning surface.

Figure 14 shows under high magnification an aggregate of burning aluminium oxide particles on a propellant surface. Wrinkles on the oxide skin are clearly indicated. Under higher magnification, cracks were also observed (Figs 15 & 16), and molten aluminium metal was exudating through these ruptures on the skins of oxide particle aggregates which formed structures looking like grape bunches (see Figs 16 & 17).

On the burning aluminized propellant the surface of AP particles were concave and dish-like, and in some cases the particles were almost flattened or almost totally consumed (Fig 18). X-ray elemental image analysis coupled with SEM showed clearly the presence of surface and sub-surface aluminium particles in the burning propellant (see Fig 18).

4. Discussion

4.1 Burn Rate Enhancement and Relative Catalyst Effectiveness

The burn rate enhancements observed in the present study are not proportional to the catalyst concentrations. In addition, at some catalyst concentrations a burn rate plateau is observed over a pressure range from approximately 8 to 14 MPa. This burn rate / concentration non-proportionality effect is in agreement with an early study on copper chromite catalysis in HTPB/AP propellants [24]. As the catalyst levels increase, the burn rate augmentations may reach a limiting value [1,6,7,36,37]. This diminishing return effect has been observed for liquid ferrocene derivative catalysts [7]. One of the causes has been attributed to catalyst agglomeration which effectively reduces its specific surface area [1,6,36,37], although it is difficult to apply the same explanation for the case of liquid ferrocenes. It has been argued [24] that the limiting concentration effect for copper chromite catalyst is a manifestation of the binder degradation being the rate-determining step in propellant combustion.

Hycat-6 and Catocene catalyse the propellant burn rates to the same extent. This is not surprising because the two catalysts are chemically analogous. Small differences in ligand substitutions in chromium complex catalysts were not found to give rise to markedly different burn rates [24].

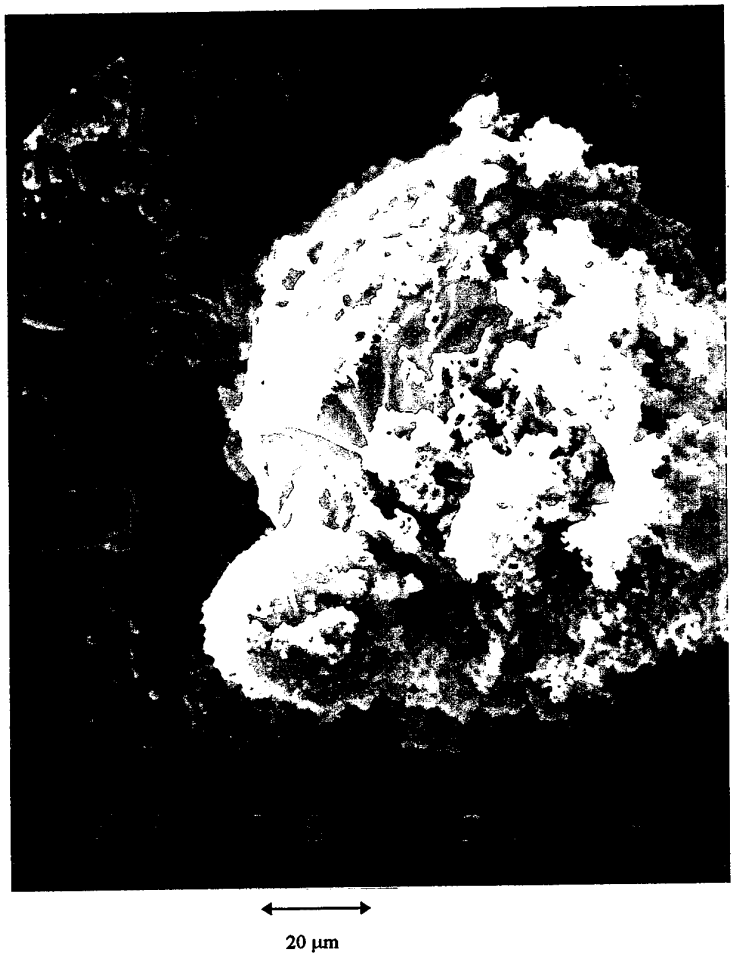

Figure 14: SEM photographs of an aluminized AP/HTPB propellant burning at 3 MPa, showing wrinkles on the aluminium oxide skin (magnification 750.

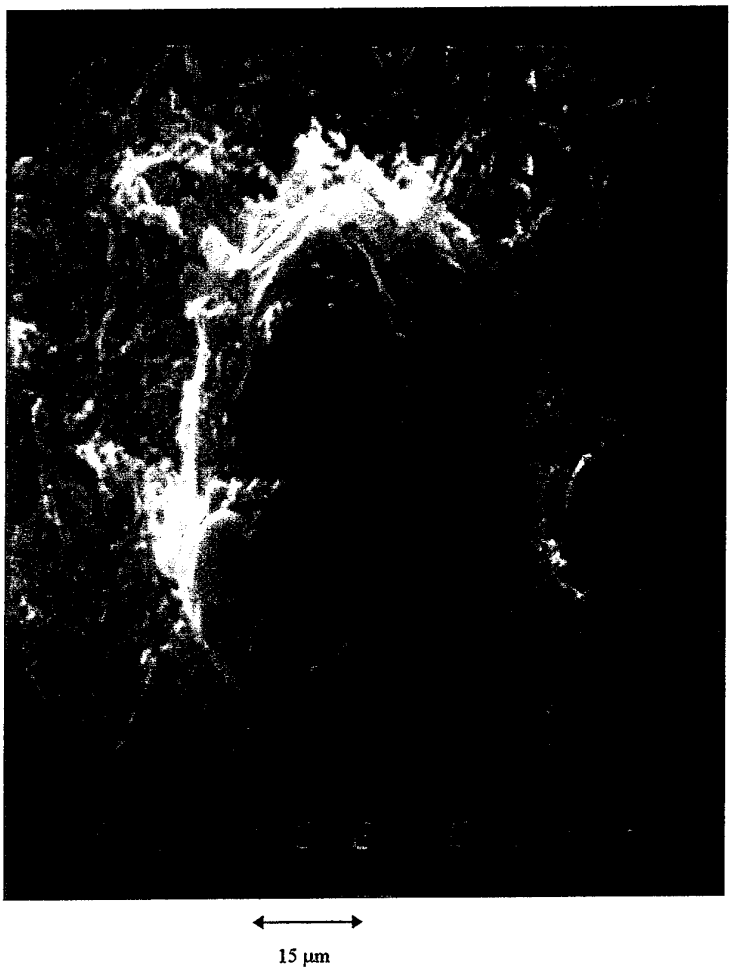

Figure 15: SEM photographs of an aluminised AP/HTPB propellant burning at 3 MPa, showing cracks on the oxide skin and exudation of molten aluminium metal (magnification 1000).

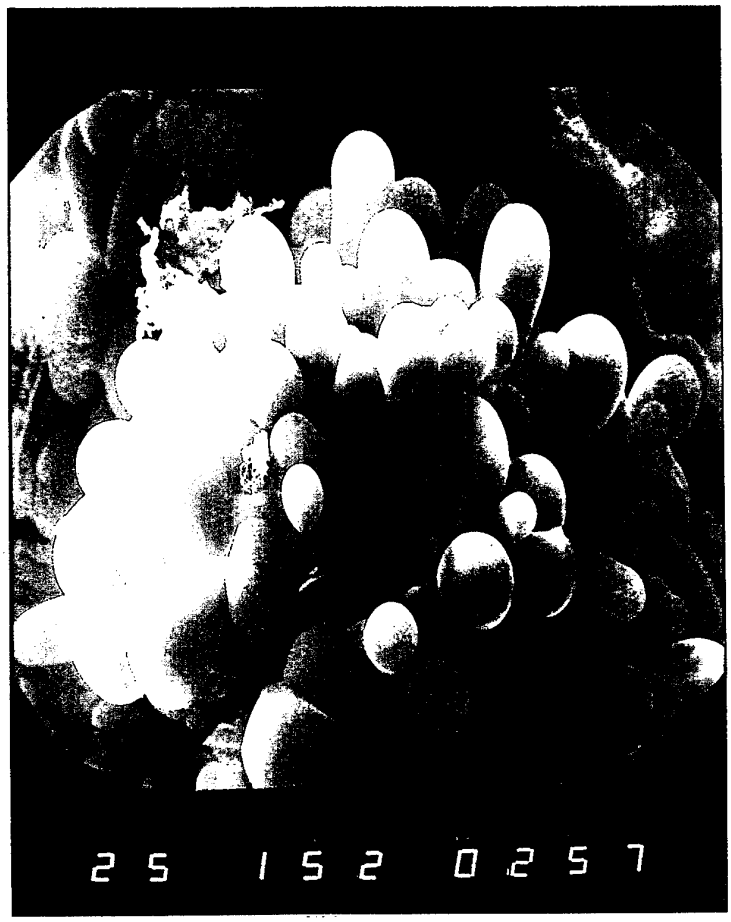

Figure 16: SEM photographs of an aluminized AP/HTPB propellant burning at 3 MPa, showing exudation of molten aluminium metal from the grape-like structure of an aggregation of aluminium particles (magnification 1500).

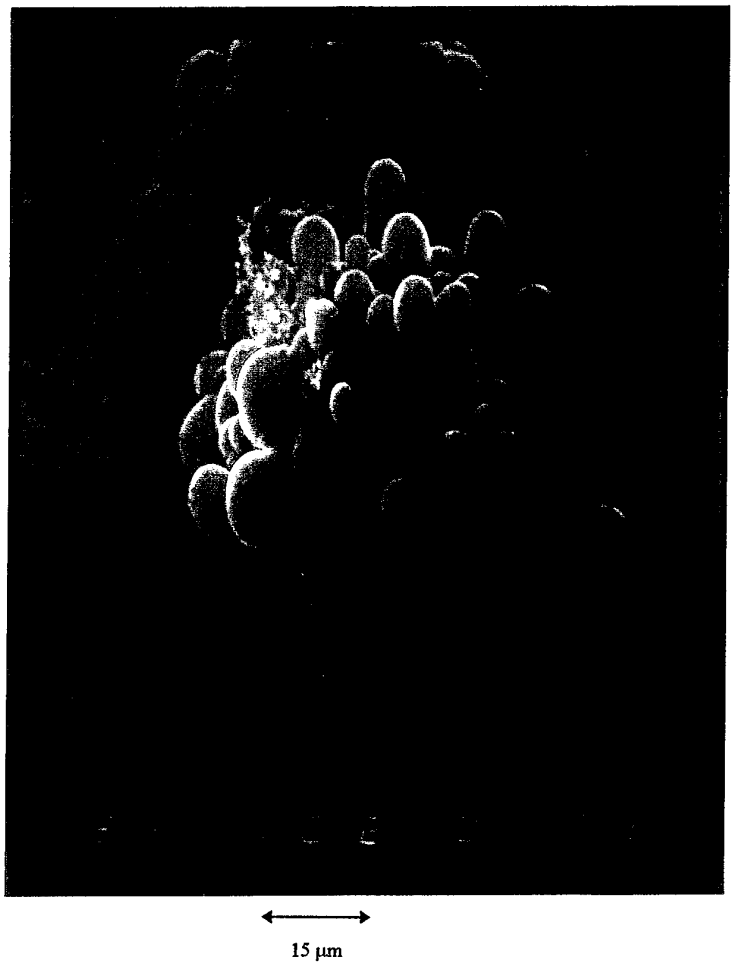

Figure 17: SEM photographs of an aluminized AP/HTPB propellant burning at 3 MPa, showing exudation of molten aluminium metal (magnification 1000).

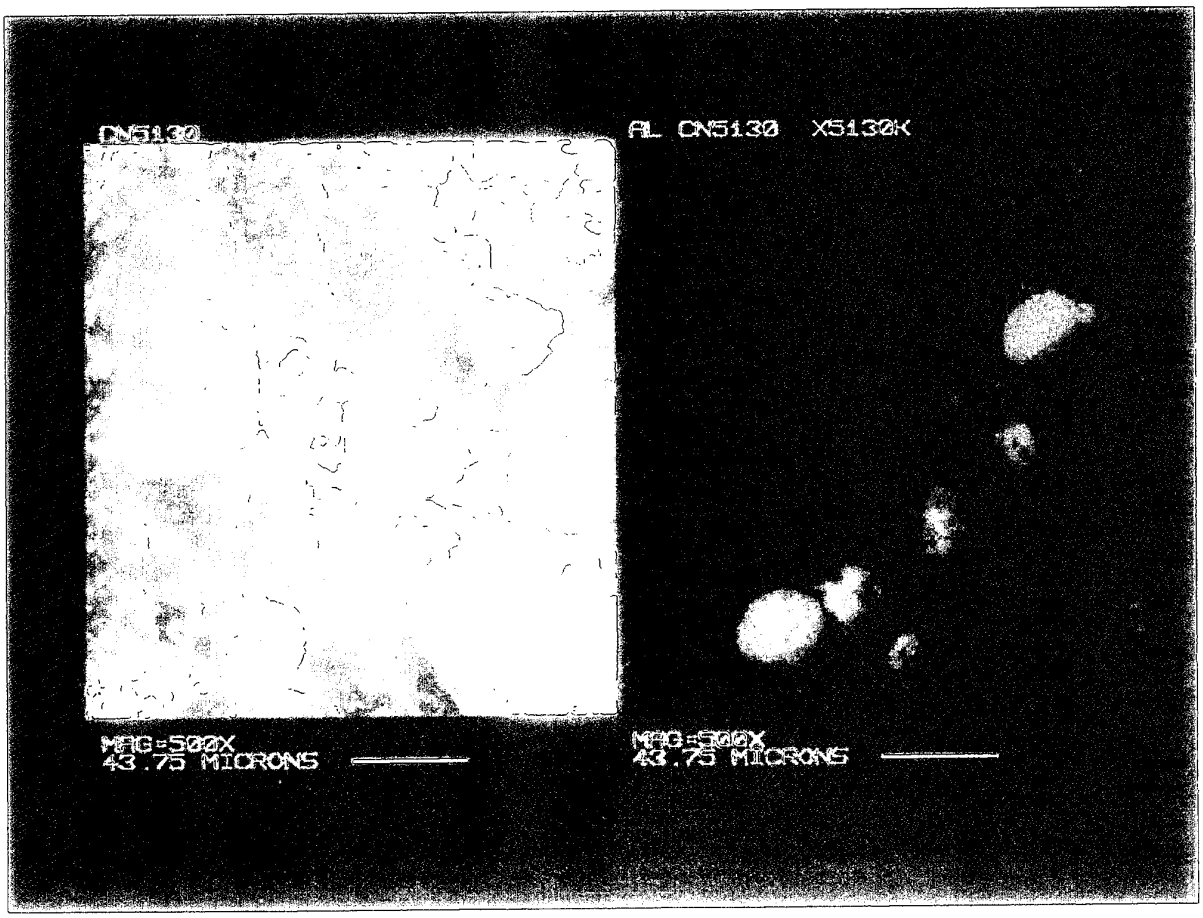

Figure 18: SEM (left) showing the burning surface of an aluminized AP/HTPB propellant; and X-ray elemental image analysis (right) showing the presence of aluminium particles on the surface and sub-surface of the burning propellant.

Butacene containing propellants display considerably higher burn rates than the corresponding Catocene propellants containing the same amounts of iron; the effect of 0.5% Butacene is approximately equivalent to that of 1% Catocene in enhancing burn rates (see Fig. 6). As noted before, Butacene contains a ferrocenic derivative grafted onto the HTPB polymer backbone. The substantial burn rate augmentation by Butacene compared to Catocene offers strong evidence that the ferrocenic catalyst functions more effectively when it is immobilized directly to the binder. Evidence for the ferrocenic catalysts acting in the binder and the mechanism of ferrocenic catalysis will be discussed in the following section.

Catocene combined with PAP appears to be the most effective of all the catalysts examined. Incorporation of 10% PAP to 1% Catocene results in almost a three-fold increase in burn rates. While fine AP (20 μm particle size) may be regarded as a burn rate enhancing catalyst, and often used in bimodal AP-based propellant to adjust burn rates in other studies, the material is not as porous as PAP. The high porosity of PAP is expected to give rise to substantially more binder/oxidiser contacts which are important for catalysis along the binder/oxidiser boundaries. These findings offer support to the conclusion regarding the active sites of the ferrocenic catalyst (see later). PAP as an oxidiser alone showed sensitisation of the exothermic decomposition temperature with increasing pressure, when compared to AP oxidiser. Addition of PAP, as partial substitution for AP, in the propellant containing Catocene did not result in sensitisation of the oxidiser decomposition, when compared to the Catocene containing propellant or to the PAP containing propellant (Figure 10). This finding is consistent with the increased temperature sensitivity of burn rates of the propellant containing Catocene with added PAP [30].

Carborane-type catalysts are very poor catalysts. There is little burn rate enhancement for NHC-containing propellants, even at 3% catalyst concentration.

Addition of aluminium in the presence of catalyst suppressed the burn rates when compared to the corresponding non-aluminized, catalyzed propellants. The net effect of aluminium addition on burn rate has been reported to be small, and it can be positive or negative [36]. In our propellants, while the ratio of the medium sized/small sized AP fractions was kept constant, i.e. 65/35, the effect of adding aluminium was to lower the overall AP/binder ratio and reduce the overall proportion of small sized AP fraction. This shift to a more fuel-rich formulation is expected to reduce the burn rate. In addition, other causes resulting from the combustion behaviour of aluminium may also be operative. The scenario of agglomeration and ignition of aluminium particles has been well-examined by Price [36] and Renie and Osborn [37]. Because combustion of aluminium particles may still continue after their detachment from the burning surface, much of the heat release probably occurs too far from the surface to affect the heat feedback, thus contributing little to enhancing the burn rates.

An order of relative catalyst effectiveness may be established, based on observed burn rates at 20°C and 1% catalyst concentration in the same binder/oxidiser formulation.

Background $\approx$ o-Carborane $\approx$ NHC $<<$ Catocene $\approx$ Hycat-6 $<$ Butacene $<$ (Catocene + 10% PAP)

Note that this ranking is only a practical one and has no regard to whether the catalyst is a solid or liquid. As mentioned earlier, this relative assessment is a necessary precursor to a more detailed investigation on burn rate temperature sensitivity [30].

Irrespective of whether the catalyst is a good burn rate enhancer or not, the exothermic decomposition of AP in the propellant containing o-Carborane, NHC, Catocene, or Butacene, is sensitized with increasing pressure (greater than 4 MPa) when compared to that of pure AP. The addition of 10% PAP, alone or in conjunction

with 1% Catocene, does not result in sensitisation of AP thermal decomposition, although Catocene combined with PAP gives the most burn rate enhancing effect.

The experimental results demonstrate that the ease with which AP thermal decomposition takes place in the propellant does not correlate with the catalytic enhancement on propellant burn rate. It follows that AP decomposition reactions are probably not the main driving force in determining the catalyzed burn rate. Additives which do not augment propellant burn rates may still sensitize exothermic AP decomposition in the propellant.

4.2 Mechanism of Ferrocene-Catalyzed Combustion

As pointed out in the Introduction, it has been suggested that catalysts primarily act in the binder rather than directly on the AP. In the present study, strong evidence exists that the ferrocenic catalysts act in the binder to catalyze heterogeneous reactions between the binder HTPB and oxidiser AP at the binder / oxidiser interface.

The experimental evidence consists of the following

(i) Enhanced burn rates of Butacene propellants over Catocene propellants;
(ii) Fe particles observed in the HTPB binder of the quenched propellant surface;
(iii) Undercuttings along the boundary of surface AP particles of the quenched propellant; and
(iv) the convex, protruding shape (sometimes apparently intact) of AP particle surface of the quenched propellant.

There was no evidence that the catalysts promoted surface AP decomposition reactions.

(i) Enhanced Burn Rate of Butacene Propellant Compared with Catocene Propellant

As discussed earlier, the burn rate of Butacene propellants was markedly enhanced over that of Catocene propellants containing the same amounts of iron in the ferrocenic catalyst. Quite different to the Catocene molecule which possesses two ferrocenic units, the Butacene has a single ferrocenic derivative grafted on to the backbone of the pre-polymer HTPB (Figure 5). This immobilisation helps avoid the problems of vapourisation and migration of the iron catalyst into the liner or to the surface of the grain [38].

Catocene is a good burn rate enhancing catalyst, but Butacene promotes even faster burn rates. This clearly indicates the ferrocenic catalyst functions more effectively when it is firmly bound to the binder. Thus the primary catalytic action sites are in the binder, and the catalyst is likely to promote binder / oxidiser interfacial reactions.

(ii) Iron Particles Observed in the Binder

As shown in Fig 13, vigorous decomposition reactions of the ferrocenic catalyst took place in the burning propellant. X-ray elemental image analysis indicates the existence of iron containing particles dispersed in the binder of the quenched Catocene containing propellant (see Fig 19). XPS of the same propellant confirmed the presence of iron and suggested it is iron oxide, in the form of Fe_2O_3 and/or Fe_3O_4.

Oxidation of ferrocene and n-butylferrocene catalysts in burning propellants was found to yield finely divided iron (III) oxide [39]. Price and Sambamurthi [19] concluded that iron oxide catalyzes the decomposition of fuel binders to more easily oxidisable forms, thereby bringing the primary diffusion flame closer to the surface and enhancing the burn rates.

Further support can be gained from other similar observations. Wang [40] observed dispersed iron compound on the burning surface of HTPB/AP propellants and suggested the iron-containing catalysts serves as a source generating in-situ thermally stable α-Fe_2O_3 particles (>1000°C) which eject into the flame as the possible active sites. Lengele et al. [41] suggested that iron oxide increases propellant burn rates by increasing the heat flux and through direct contact with the binder.

(iii) Undercuttings Along the AP Particle Boundaries

The SEM evidence shows undercuttings around the surface AP particles. The intensity of the undercuttings appeared to be pressure dependent, and they were most pronounced at low pressures. This observation has been described previously in both propellant sandwich systems by Boggs et al. [33], and in actual propellants by Wang [40] and Krishnan et al. [16-18]. The undercuttings have been interpreted as indicating AP/binder heterogeneous interactions along the interface.

(iv) The Convex Shape of AP Particle Surface

SEM of the quenched surfaces of the Catocene and Butacene containing propellants shows the surface of AP particles to be convex, i.e. protruding from the propellant regressing surface, throughout the pressure range 2 to 10 MPa. The AP burning was lagging behind the flame front and in some instances the AP particle surface appeared almost totally intact, without any apparent significant surface activities [42]; see Figs 20a &b. Yet the burn rate of the catalyzed propellant is enhanced over the propellant containing no catalyst. Thus the ferrocenic additive, while enhancing the burn rate, does not promote surface decomposition of AP, and its action must be in the binder.

Figure 19: SEM (left) of a burning AP/HTPB propellant containing a ferrocenic catalyst at 3 MPa; and X-ray elemental image analysis (right) showing the presence of reacting iron particles (from the catalyst) dispersed in the binder.

(a)

Figure 20: SEM photographs of a burning AP/HTPB propellant at 2 MPa; (a) the propellant containing no catalyst; and (b) the propellant containing 0.5% Catocene catalyst.

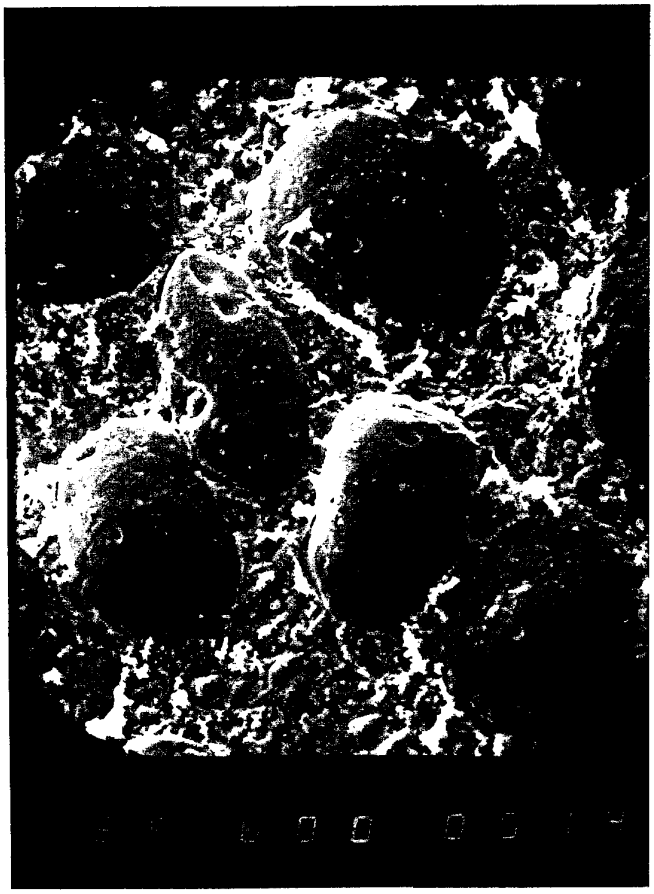

(b)

Figure 20 (Contd): SEM photographs of a burning AP/HTPB propellant at 2 MPa; (a) the propellant containing no catalyst; and (b) the propellant containing 0.5% Catocene catalyst.

In sharp contrast, for the propellants without catalyst, the AP particle surface was concave, i.e. dish-like, with white, intensely frothy areas at the middle of the particle, indicating surface decomposition reactions yielding gaseous products.

Theoretical calculations in parallel with the present experiments confirmed that in the Catocene containing propellant the binder burns faster than the AP particle surface at both low (2 MPa) and high (7 MPa) pressures [42]. Bilger and Jia [43] conclude that it is the diffusion process which has a strong influence on the combustion of mid-sized AP (80 μm) and the HTPB binder, while the combustion of coarse-sized AP (400 μm) simply behaves like monopropellant AP combustion.

By contrast, the shapes of AP particle surface on the propellants containing carborane catalysts were found to be both convex and concave. The AP and the binder burn effectively at the same rate, and this is consistent with the fact that the carborane catalysts showed little burn rate enhancement. On the uncatalysed propellant surface, the exothermic decomposition of AP was the driving force for propellant burning, and the concave, dishlike surface of the AP particles with white, frothy areas at the middle of the particles were indicative of oxidiser initiation surface reactions.

4.3 Primary Diffusion Flame Control

All the evidence presented above strongly indicates that the ferrocenic catalyst acts in the binder, not in the AP, to promote the heterogeneous binder/AP reactions along the AP particle boundaries. Such reactions at the binder / oxidiser interface would catalyze the primary diffusion flame because of the close proximity of the flame to the interface. The final diffusion flame would be too far removed from the burning surface, whereas the AP monopropellant flame would be geometrically inaccessible to the catalyst particles.

Beckstead, in his pioneering work on the theoretical model of composite propellant combustion, explained [44] the shape of the primary diffusion flame. In the initial stage of the combustion, a fuel-rich environment exists, and the primary flame shape closes over the oxidiser crystal surface. As the combustion reaches a steady state and the AP particle is exposed to a more oxidiser-rich environment, the shape of the primary flame would close over the binder, crossing the binder/oxidiser boundary. This configuration would enhance the interaction between the primary diffusion flame and the interfacial binder/oxidiser reaction products. The importance of such configuration of the primary diffusion flame has recently been re-affirmed by Beckstead [45].

Figure 21 depicts an environment surrounding an AP surface particle in which the binder/AP reactions occurring at the interface enhances the primary diffusion flame. The convex, protruding shape of the AP particle surface together with the undercuttings along the AP particle boundaries clearly suggest that the dominant heat feedback to the burning surface is from the primary diffusion flame. Most of the heterogeneous reaction products between the binder and the AP would be readily fed into the primary flame. Had AP condensed-phase decomposition reactions been of significance, these reaction products would have energized the AP monopropellant flame which would have in turn resulted in significant heat feedback and caused the AP particle surface shape to be recessed at the middle [46], rather than protruding and convex as consistently observed in the present study.

The combustion which is driven by the diffusion flame is less temperature sensitive than that by the AP flame [47]. This notion is consistent with the theoretical view that the diffusion processes are less temperature sensitive than the kinetic processes, bearing in mind that the AP flame is a kinetically limited flame. To reduce burn rate temperature sensitivity it is therefore desirable to have diffusion flame control. In the present study, both Catocene and Butacene are found to be effective in reducing this

temperature dependence [30], lending further support to the contention of Beckstead and Cohen [48] that the ferrocene-catalysed combustion is diffusion flame controlled.

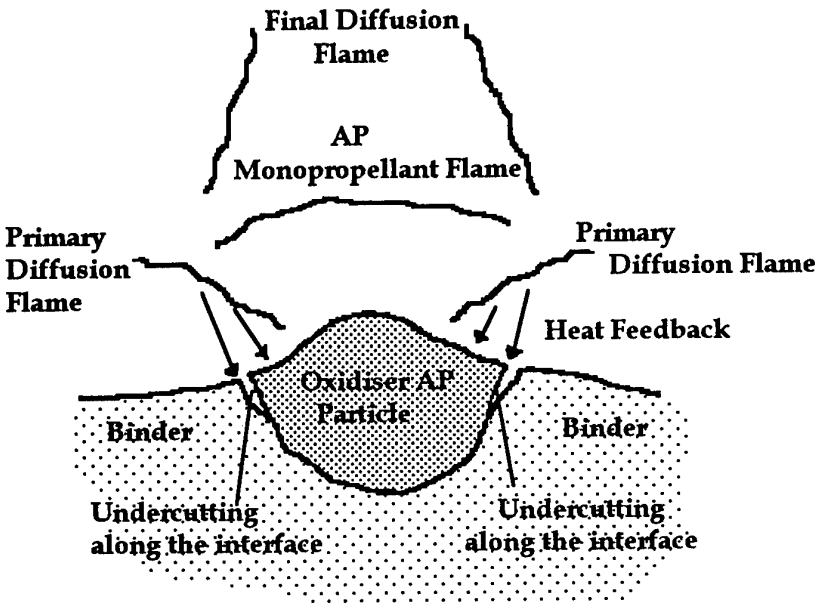

Figure 21: Combustion flame model of a ferrocene-catalysed AP/HTPB propellant showing the convex, protruding AP particle surface, undercuttings along the oxidiser/binder interface, and the primary diffusion flame bending across the interface.

4.4 Metal Additives on the Burning Surface

(i) Aluminium Particles

In the present study, significant SEM evidence showed the actual exudation of molten aluminium through cracks in the oxide skins. Although aluminium agglomerates on propellant burning surfaces have been reported in previous studies [36], the protrusion and expansion of molten aluminium through cracks on the oxide skins were only observed in laboratory tests under simulated conditions.

There are a number of factors causing fractures of metal oxide skins [36], an important requirement being that the ratio of thermal expansion coefficients of metal to metal oxide be greater than unity. Aluminium oxide (Al_2O_3) melts at too high a temperature (2045°C), but the melting point of aluminium metal is sufficiently low (660°C) under propellant burning surface conditions (700 - 900°C) to enable the exudation of molten aluminium.

The formation of aluminium oxide skins tends to delay or inhibit ignition of aluminium which is inherently slow to vaporize at propellant surface temperatures. When combustion of aluminium does take place, much of the heat release occurs too far from the burning surface [38] to enhance the burn rate. This behaviour explained the observed suppressed burn rates of aluminized propellants compared to the non-aluminized ones.

Aluminium particles on the propellant burning surface have been previously treated either as a heat sink or a heat source [37]. The heat sink effect would increase the burn rate temperature sensitivity, but the heat source effect would reduce it. Results on the burn rate temperature sensitivity of aluminized propellants [30] tend to suggest that in these propellant formulations the aluminium particles function as a heat sink.

(ii) Iron Particles

The SEM of quenched ferrocenic propellants showed white frothy aggregations of iron containing compounds, and the XPS Fe 2p spectra suggested the compounds were most likely to be iron oxides. This provides experimental confirmation of the previous conclusion that ferrocene and n-butylferrocene undergo oxidation in burning propellants to produce iron (III) oxide [39]. It was suggested [19] that iron oxide catalyses the decomposition of fuel binders to more oxidisable forms, thereby bringing the primary diffusion flame closer to the surface and enhancing propellant burn rates. This suggestion is supported by the present findings that the primary diffusion flame plays a dominant role in burn rate enhancement by ferrocenic catalysts.

It was suggested that particles of the much more thermally stable iron oxide, in the form of Fe(II)O (melting point 1380°C) could serve as catalytic active sites in the flame [40], although this contention has yet to be supported by experimental evidence.

The behaviour of iron particles is in contrast to the behaviour of aluminium particles discussed above. The exothermic decomposition reactions of iron compounds, the enhanced burn rates of the ferrocene-catalyzed propellants, and their reduced temperature sensitivity [30], lend support to the contention that the iron particles function as a heat source, releasing energy from the vigorous reactions to significantly affect the heat feedback to the burning surface.

5. Summary and Conclusion

The present study has examined the combustion of HTPB/AP propellants containing ferrocenic and carborane-type burn rate catalysts. The carborane-type catalysts show little enhancement of burn rates, even up to 3% catalyst concentration. The ferrocene-type catalysts are good burn rate enhancers. In particular, Catocene and Butacene show substantial enhancements. At 1% Catocene, the burn rate increase is approximately 100% throughout the effective rocket operational pressure range. Butacene propellants

containing the same amount of iron as Catocene propellants were shown to possess higher burn rates than the Catocene propellants.

At 1% catalyst concentration, a relative order of catalytic effectiveness in terms of propellant burn rates is established:

Uncatalysed ≈ o-Carborane ≈ NHC << Catocene ≈ Hycat-6 < Butacene < Catocene+10% PAP).

The present results provide strong evidence in favour of the ferrocenic catalyst acting in the binder to catalyze the heterogeneous reactions between the binder and oxidiser AP at the oxidiser / binder interface.

The experimental evidence consists of the following:

(i) Enhanced burn rates of the Butacene propellants compared to the Catocene propellants,

(ii) Fe particles were found to be dispersed in the binder of the quenched propellant,

(iii) Undercuttings along the boundary of the surface AP particles in the quenched propellant, and

(iv) Protruding, convex (sometimes apparently intact) shape of surface AP particles in the quenched propellant.

There was little evidence of the ferrocenic catalyst enhancing the decomposition of AP on the burning propellant surface. The heterogeneous binder/oxidiser reactions are most likely to occur in the condensed phase at the binder/oxidiser interface. There was no experimental evidence for the catalyst enhancing the binder/oxidiser reactions in the gas phase. Under the burning surface conditions and due to the close proximity of the primary flame to the binder/oxidiser interface, the ferrocene-catalyzed combustion is controlled by the primary diffusion flame.

It is shown that the iron oxides formed in-situ from the ferrocenic catalyst undergo vigorous exothermic decomposition on the burning surface. Fresh evidence on the aluminized propellant surface shows the actual exudation of molten aluminium metal through cracks on the aluminium oxide skins.

6. Acknowledgments

The technical assistance of Peter Berry, of the DSTO Weapons Systems Division, in processing the propellants, operating the interrupt bomb, and in data reduction is acknowledged. Graham Fowler, of the DSTO Land, Space and Optoelectronics Division, is thanked for collecting the SEM and related data.

7. References

1. Kishore, K., and Sunitha, M.R., AIAA J. 17:118-1125 (1979).

2. Beckstead, M.W., 18th Symposium (Intern) on Combustion, The Combustion Institute, Pittsburgh, 1981, pp.175-185.

3. Kishore, K., AIAA J. 17:1216-1224 (1979).

4. Kishore, K. and Gayathri, V., Ignition and Combustion of AP-based Propellants, in Fundamentals of Solid Propellant Combustion, Edts. Kuo, K. and Summerfield, M., Series "Progress in Astronautics and Aeronautics", 90:53-119 (1984).

5. Cohen, N.S., Fleming, R.W., and Derr, R.L., AIAA J. 2:212-218 (1974).

6. Cohen, N.S., AIAA J. 18:277-293 (1980).

7. Pittman, C.U., AIAAJ. 7:328-334 (1969).

8. Burnaside, C.H., AIAA Paper 75-234 (1975).

9. Pearson, G.S., Combustion Sci. Tech. 3:155-163 (1971).

10. Bakhman, N.N., Nikiforov, V.S., Avdyunin, V.I., Fogelzang, A.E., and Kichin, Y.S., Combust Flame 22:77-87 (1974).

11. Rastogi, R.P., Singh, G., and Singh, R.R., Combust Flame 30:117-124 (1977).

12. Beckstead, M.W. and Hightower, J.D., AIAA J. 5:1785-1790 (1967).

13. Selzer, H. The 11th Symp (Intern) Combustion, The Combustion Institute, Pittsburgh, 439-446 (1967).

14. (a) McGurk, J.L., "Crystallographic Changes in AP Related to Different Rates of Heating", Proc of 3rd Interagency Chemical Rocket Propulsion Group (ICRPG) Combustion Conf., Chemical Propulsion Information Agency (CPIA), Publ. No. 138, pp. 51-62, Feb 1967.
(b) McGurk, Microscopic Determination of Propellant Combustion Surface Temperature, Proc of 1st InterAgency Chem Rocket Prop Group Combus Instability Conf., CPIA Pub. No. 68, pp. 345-359, Jan 1965.

15. Kumar, R.N., "Condensed Phase Details in the Time Dependent Combustion of AP Composite Propellants", Combustion Sci. & Technol., Vol8, pp. 133-148, 1973.
Kumar, R.N., "A New Look at AP/Composite Propellants", JPL Quarterly Technical Rev., Vol 3, pp. 53-77, July 1973.

16. Krishnan, S., and Periasamy, C., AIAA J. 24:1670-1675 (1986).

17. Krishnan, S. and Jeenu, R., Combustion and Flame 80: 1-6 (1990).

18. Krishnan, S., and Jeenu, R., J. Propulsion and Power 8:748-755 (1992).

19. Price, E.W. and Sambamurthi, J.K., CPIA Publication 412, Chemical Propulsion Information Agency, John Hopkins University, Baltimore, MD, Vol 1 (1981).

20. Hightower, J.D. and Price, E.W., Astronaut. Acta 14:11-21 (1968).

21. Kishore, K., Pai Veneker, V.R., Chaturvedi, B.K., and Gayathri, V., AIAA J. 15:114-116 (1977).

22. Kishore, K., Pai Veneker, V.R. and Gayathri, B.K., Fuel 60:164-167 (1981).

23. Sammons, G.D., Analytical Chem. Plennum Press, New York, 305-311 (1968).

24. Fong, C.F. and Hamshere, B.L. Combust Flame 65:61-69 (1986).

25. Nadaud, L., Combust Flame 12:177-195 (1968).

26. Jones, H.E. and Strahle, W.C., "Effect of Copper Chromite and Iron Oxide Catalysts on AP/CTPB Sandwich", Proceedings of the 14th Symposium (International) on Combustion, The Combustion Institute, Pittsburgh, 1287-1295 (1972).

27. Boggs, T.L., Zurn, D.E., Cordes, H.F., and Covino, J., J. Propulsion Power 4:27-40 (1988).

28. Inami, S.H., Rajapakse, Saw, R., and Wise, H., Combust Flame 17:189-196 (1971).

29. Nguyen, T.T., DSTO Materials Research Laboratory, Technical Report "Burn Rate Temperature Sensitivity of Solid Rocket Propellants: An Overview of Current Status of Experimental Results", MRL-TR-92-5 (1992).

30. Nguyen, T.T. , "Reduced Burn Rate Temperature Sensitivity of Ferrocene-Catalysed Combustion of AP/HTPB Composite Solid Propellants". To be published in J. Energetic Materials.

31. Klager, K., Mansfred, R.K., and Lista, E.L., "Burning Behaviour of Porous Ammonium Perchlorate", Proceedings of the ICT pp. 283-297 (1979).

32. (a) Kilpin, D. and Jolley, W.H., "A Window Bomb for Propellant Combustion Studies", WRSL-TM-28/91. (b) Boggs, T.L., Crump, J.E., Krateutle, K.J., and Zurn, D.E.,"Cinephotomicrography and Scanning Electron Microscopy as Used to Study Solid Propellant Combustion", in "Experimental Diagnostics in Combustion of Solids", in the Series "Progress in Astronautics and Aeronautics", 63:20-48 (1978), The American Institute of Astronautics and Aeronautics, New York.

33. Sharma, J. and Beard, B.C., "Fundamentals of X-Ray Photoelectron Spectroscopy (XPS) and its Application to Explosives and Propellants", in " Chemistry and Physics of Energetic Materials", Edt. S.N. Bulusu, Kluwer Academic Publishers, The Netherlands, pp 569-585 (1990).

34. Boggs, T.L., Derr, R.L., and Beckstead, M.W., Surface Structure of Ammonium Perchlorate Composite Propellants, AIAA J., 8:370-372 (1970).

35. Shannon, L.J. AIAA J. 8:346-353 (1970).

36. Price, E.W. Combustion of Metallized Propellants, in "Fundamentals of Solid Propellant Combustion", Edts. Kuo, K. and Summerfield, M., in Series "Progress in Astronautics and Aeronautics", 90:479-513 (1984).

37. Rennie, J.P. and Osborn, J.R. the 16th Joint Propulsion Conference, AIAA Paper 80-1116 pp. 1-15 (1980).

38. Finck, B. and Mondet, J.C. The 19th Intern. Annual ICT Conference, Karlsruhe, Germany (1988).

39. Flanigan, D.A., Air Force Rocket Propulsion Laboratory Technical Report AFRPL-TR-67-18 (1967).

40. Wang, S.Y., Wang, S.S., Liu, F., and Chiu, H.S., "Investigation of Catalysis in the Combustion of Iron Catalyzed Composite Propellants", Proc. Intern. Annual Conference ICT, pp-8-1 to 8-14 (1988).

41. Lengelle, G., Brulard, J., and Moutet, H., 16th Symp (Intern) Combustion, pp. 1257-1269 (1976).

42. Bilger, R.W., Jia, X., and Nguyen, T.T., "Mechanism of AP-Based Composite Propellant Combustion", submitted to J. Combust. Sci. Technology (1994).

43. Bilger, R.W. and Jia, X., "The Burke Schumann Diffusion Flame with Zero Net Flux Boundary Conditions", J. Combust. Sci. Technology (1994) in press.

44. Beckstead, M.W., "Ballistic Control of Solid Propellants. Vol III. Description of the Separate Surface Temperature Model for Solid Propellant Combustion", AFRPL-TR-81-58, Air Force Rocket Propulsion Laboratory, 1982.

45. Beckstead, M.W., "Solid Propellant Combustion Mechanism and Flame Structure", Pure & Applied Chemistry, 65:297-307 (1993).

46. Quinn Brewster, M. , Annual Review of Heat Transfer, Chapt 6, pp. 287-330 (1992).

47. Cohen, N. and Flanigan, D.A., AIAA J., 23:1538-1547 (1985).

48. Beckstead, M.W. , and Cohen, N., 7th JANNAF Combustion Meeting, CPIA Publication 204, Vol II, pp.75-84 (1971).

The Effects of Ferrocenic and Carborane Derivative Burn Rate Catalysts in AP Composite Propellant Combustion: Mechanism of Ferrocene-Catalysed Combustion

T.T. Nguyen

(DSTO-TR-0121)

DISTRIBUTION LIST

DEFENCE ORGANISATION

Defence Science and Technology Organisation

Chief Defence Scientist
FAS Science Policy } shared copy
AS Science Corporate Management
Counsellor Defence Science, London (Doc Data Sheet only)
Counsellor Defence Science, Washington (Doc Data Sheet only)
Scientific Adviser to Thailand MRD (Doc Data Sheet only)
Scientific Adviser to the DRC (Kuala Lumpur) (Doc Data Sheet only)
Senior Defence Scientific Adviser/Scientific Adviser Policy and Command (shared copy)
Navy Scientific Adviser (3 copies Doc Data Sheet and 1 copy of distribution list)
Scientific Adviser - Army (Doc Data Sheet only)
Air Force Scientific Adviser
Director Trials

Aeronautical and Maritime Research Laboratory

Director, AMRL
Chief, Weapons Systems Division
Dr T.T. Nguyen 3 copies
Dr J. Adams
Dr R.J. Spear
Dr B. Thorpe
Dr J. Gardner
B.L. Hamshere
J.F. Hooper
Dr W. Jolley
D. Kilpin
S. Odgers
M. Chick
N. Ayres

DSTO Library

Library Fishermens Bend
Library Maribyrnong
Main Library DSTOS (2 copies)
Library, MOD, Pyrmont (Doc Data Sheet only)

Defence Central

OIC TRS, Defence Central Library
Officer in Charge, Document Exchange Centre, 12 copies

DISTRIBUTION LIST (Contd)

Defence Intelligence Organisation
Library, Defence Signals Directorate (Doc Data Sheet only)

Army

Director General Force Development (Land) (Doc Data Sheet only)
ABCA Office, G-1-34, Russell Offices, Canberra (4 copies)
NAPOC QWG Engineer NBCD c/- DENGRS-A, HQ Engineer Centre

Navy

Director General Force Development (Sea), (Doc Data Sheet)
DNW, Maritime Headquarters, Pott Points, NSW

UNIVERSITIES AND COLLEGES

Australian Defence Force Academy
Library
Head of Aerospace and Mechanical Engineering
Deakin University, Serials Section (M list), Deakin University Library, Geelong, 3217,
Senior Librarian, Hargrave Library, Monash University
Professor J. Mackie, Department of Physical and Theoretical Chemistry, Sydney University
Professor R. W. Bilger, Department of Mechanical and Mechatronic Engineering, Sydney University

OTHER ORGANISATIONS

NASA (Canberra)
AGPS

ABSTRACTING AND INFORMATION ORGANISATIONS

INSPEC: Acquisitions Section Institution of Electrical Engineers
Library, Chemical Abstracts Reference Service
Engineering Societies Library, US
American Society for Metals
Documents Librarian, The Center for Research Libraries, US

INFORMATION EXCHANGE AGREEMENT PARTNERS

Acquisitions Unit, Science Reference and Information Service, UK
Library - Exchange Desk, National Institute of Standards and Technology, US

SECURITY CLASSIFICATION OF THIS PAGE **UNCLASSIFIED**

REPORT NO.	AR NO.	REPORT SECURITY CLASSIFICATION
DSTO-TR-0121	AR-009-173	UNCLASSIFIED

TITLE

The effect of ferrocenic and carborane derivative burn rate catalysts in AP composite propellant combustion: Mechanism of ferrocene-catalysed combustion

AUTHOR(S)
T.T. Nguyen

CORPORATE AUTHOR
DSTO Aeronautical and Maritime Research Laboratory
PO Box 4331
Melbourne Victoria 3001

REPORT DATE	TASK NO.	SPONSOR
August 1995	DST 92/309	DSTO

FILE NO.	REFERENCES	PAGES
510/207/0042	48	47

CLASSIFICATION/LIMITATION REVIEW DATE

CLASSIFICATION/RELEASE AUTHORITY
Chief, Weapons Systems Division

SECONDARY DISTRIBUTION

Approved for public release

ANNOUNCEMENT

Announcement of this report is unlimited

KEYWORDS

Propellant combustion	X-ray photoelectron spectroscopy	Propellant burn out
Burning time	Composite propellants	Ammonium perchlorate
Catalysts	Aluminized propellants	Explosives
Pyrolysis	Scanning electron microscopy	Solid rocket propellants

ABSTRACT

The combustion of HTPB/AP propellants containing ferrocene-type and carborane-type burn rate catalysts was examined. The ferrocenic catalysts are good burn rate enhancers, but the carborane-type compounds showed little improvement, even at 3% catalyst concentration. An order of relative catalyst effectiveness was established for 1% catalyst concentration at 20°C. Examination reveals the enhancing effect of 1% Catocene is approximately equivalent to 0.5% Butacene. Characteristic surface features observed for the carborane-catalysed propellants contrast to those for the ferrocene-catalysed propellants. For ferrocene-catalysed combustion, the experimental evidence is in favour of a mechanism whereby the ferrocenic catalyst acts in the binder to catalyse the heterogeneous reactions between the binder and the AP at the binder/oxidiser interface. The evidence includes the following: (i) Enhanced burn rates of the Butacene propellant over the Catocene propellant, both propellants containing the same amount of iron in the ferrocenic catalysts; (ii) Fe particles dispersed in the binder of the quenched propellant surface; (iii) undercuttings along the boundaries of surface AP particles; and (iv) the convex, protruding (sometimes apparently intact) AP particle surface. There was no evidence of the catalyst promoting surface AP decomposition reactions.